

1        **The interpretation of temperature and salinity variables in numerical**  
2        **ocean model output, and the calculation of heat fluxes and heat content**

4                                    by

6                    Trevor J. McDougall<sup>1</sup>, Paul M. Barker<sup>1</sup>, Ryan M. Holmes<sup>1,2</sup>,  
7                    Rich Pawlowicz<sup>3</sup>, Stephen M. Griffies<sup>4</sup> and Paul J. Durack<sup>5</sup>

9        <sup>1</sup>School of Mathematics and Statistics,  
10        University of New South Wales, Sydney, NSW 2052, Australia

11        <sup>2</sup>Australian Research Council Centre of Excellence for Climate Extremes,  
12        University of New South Wales, Sydney, NSW 2052, Australia

13        <sup>3</sup>Dept. of Earth and Ocean Sciences, University of British Columbia,  
14        Vancouver, B.C. V6T 1Z4, Canada

15        <sup>4</sup>NOAA/Geophysical Fluid Dynamics Laboratory, and Princeton University  
16        Atmospheric and Oceanic Sciences Program, Princeton, New Jersey, USA

17        <sup>5</sup>Program for Climate Model Diagnosis and Intercomparison, Lawrence Livermore  
18        National Laboratory, Livermore, California, USA

21        Corresponding author email: [Trevor.McDougall@unsw.edu.au](mailto:Trevor.McDougall@unsw.edu.au)

22        Full address

23        Trevor J McDougall  
24        School of Mathematics and Statistics  
25        University of New South Wales, NSW 2052, Australia  
26        tel: +61 2 9385 3498  
27        fax: +61 2 9385 7123  
28        mob: +61 407 518 183

29        keywords    ocean modelling, CMIP, ocean model intercomparison, TEOS-10,  
30        EOS-80,

32                                    Submitted to *Geoscientific Model Development*

33                                    This version is dated 6<sup>th</sup> May 2021

35 **Abstract**

36 The international thermodynamic equation of seawater of 2010 (TEOS-10) defined the  
37 enthalpy and entropy of seawater, thus enabling the global ocean heat content to be  
38 calculated as the volume integral of the product of in situ density,  $\rho$ , and potential  
39 enthalpy,  $h^0$  (with reference sea pressure of 0 dbar). In terms of Conservative  
40 Temperature,  $\Theta$ , ocean heat content is the volume integral of  $\rho c_p^0 \Theta$ , where  $c_p^0$  is a  
41 constant “isobaric heat capacity”.

42 However, many ocean models in the Coupled Model Intercomparison Project  
43 phase 6 (CMIP6) as well as all models that contributed to earlier phases, such as  
44 CMIP5, CMIP3, CMIP2 and CMIP1 used EOS-80 (Equation of State - 1980) rather than  
45 the updated TEOS-10, so the question arises of how the salinity and temperature  
46 variables in these models should be physically interpreted, with a particular focus on  
47 comparison to TEOS-10 compliant observed estimates. In this article we address how  
48 heat content, surface heat fluxes and the meridional heat transport are best calculated  
49 using output from these models, and how these quantities should be compared with  
50 those calculated from corresponding observations. We conclude that even though a  
51 model uses the EOS-80 equation of state which expects potential temperature as its  
52 input temperature, the most appropriate interpretation of the model’s temperature  
53 variable is actually Conservative Temperature. This perhaps unexpected  
54 interpretation is needed to ensure that the air-sea heat flux that leaves/arrives-in the  
55 atmosphere and sea ice models is the same as that which arrives-in/leaves the ocean  
56 model.

57 We also show that the salinity variable carried by TEOS-10 based models is  
58 Preformed Salinity, while the prognostic salinity of EOS-80 based models is also  
59 proportional to Preformed Salinity. These interpretations of the salinity and  
60 temperature variables in ocean models are an update on the comprehensive Griffies et  
61 al (2016) paper that discusses the interpretation of many aspects of coupled Earth  
62 system models.

63

## 64 1. Introduction

65 Numerical ocean models simulate the ocean by calculating the acceleration of  
66 fluid parcels in response to various forces, some of which are related to spatially-varying  
67 density fields that affect pressure, as well as solving transport equations for the two  
68 tracers on which density depends, namely heat content (or its related parameter,  
69 temperature, [the CMIP6 variables identified as  $\theta$  or  $\theta_{big}$ ])) and dissolved  
70 matter (“salinity”, [CMIP6 variable  $s_o$ ]). For computational reasons it is useful for the  
71 numerical schemes involved to be conservative, meaning that the amount of heat and  
72 salt in the ocean changes only due to the area integrated fluxes of heat and salt that cross  
73 the ocean’s boundaries; in the case of salt, this is zero. This conservative property is  
74 guaranteed for ocean models to within computational truncation error since these  
75 numerical models are designed on the basis of finite volume integrated tracer  
76 conservation (e.g., see Appendix F in Griffies et al 2016). It is only by ensuring such  
77 conservation properties that scientists can reliably make use of numerical ocean models  
78 for the long (centuries and longer) simulations required for climate and Earth system  
79 studies.

80 However, this apparent numerical success ignores some difficult theoretical  
81 issues with the equation set being numerically solved. Here, we are concerned with  
82 issues related to the properties of seawater that have only recently been widely  
83 recognized as a result of research resulting in the Thermodynamic Equation of Seawater  
84 2010 (TEOS-10). These issues mean that the intercomparison of different models, and  
85 comparison with ocean observations, needs to be undertaken with care.

86 In particular, it is widely recognized that the traditional measure of heat content  
87 in the ocean (with respect to an arbitrary reference state), the so-called potential  
88 temperature, is not a conservative variable (McDougall, 2003). Hence, the time change  
89 of potential temperature at a point in space is not determined solely by the convergence  
90 of a potential temperature flux at that point. Furthermore, the non-conservative nature  
91 of potential temperature means that the potential temperature of a mixture of water  
92 masses is not the mass average of the initial potential temperatures since potential  
93 temperature is “produced” or “destroyed” by mixing within the ocean’s interior. This

94 empirical fact is an inherent property of seawater (e.g., McDougall 2003, Graham and  
95 McDougall 2013), and so treating potential temperature as a conservative tracer (as well  
96 as making certain other assumptions related to the modelling of heat and salt) results in  
97 contradictions, which have been built into most numerical ocean models to varying  
98 degrees.

99         These contradictions have existed since the beginning of numerical ocean  
100 modelling, but have generally been ignored or overlooked because many other  
101 oceanographic and numerical factors were of greater concern. However, as global heat  
102 budgets and their imbalances are now a critical factor in understanding climate changes,  
103 it is important to examine the consequences of these assumptions, and perhaps correct  
104 them even at the cost of introducing problems elsewhere. These concerns are  
105 particularly important when heat budgets are being compared between different  
106 models, and with similar calculations made with observed conditions in the real ocean.

107         The purpose of this paper is to describe these theoretical difficulties, to estimate  
108 the magnitude of errors that result, and to make recommendations about resolving them  
109 both in current and future modelling efforts. For example, the insistence that a model's  
110 temperature variable is potential temperature involves errors in the air-sea heat flux in  
111 some areas that are as large as the mean rate of current global warming. A simple re-  
112 interpretation of the model's temperature variable overcomes this inconsistency and  
113 allows the coupled climate model to conserve heat.

114         The reader who wants to skip straight to the recommendations on how the  
115 salinity and temperature outputs of CMIP models should be interpreted can go straight  
116 to section 6.

117

## 118 **2. Background**

### 119 *Thermodynamic measures of heat content*

120         It is well-known that *in situ* temperature is not a satisfactory measure of the "heat  
121 content" of a water parcel because the *in situ* temperature of a water parcel changes as  
122 the ambient pressure changes (i.e. if a water parcel is transported to a different depth  
123 [pressure] in the ocean). This change is of order 0.1°C as pressure changes 1000 dbar,

124 and is large relative to the precision of  $0.01^{\circ}\text{C}$  required to understand deep ocean  
125 circulation patterns. The utility of *in situ* temperature lies in the fact that it is easily  
126 measured with a thermometer, and that air-sea boundary heat fluxes are to some degree  
127 proportional to *in situ* temperature differences.

128 Traditionally, potential temperature has been used as an improved measure of  
129 ocean heat content. Potential temperature is defined as the temperature that a parcel  
130 would have if moved isentropically and without exchange of mass to a fixed reference  
131 pressure (usually taken to be surface atmospheric pressure), and can be calculated from  
132 measured ocean *in situ* temperatures using empirical correlation equations based on  
133 laboratory measurements. However, the enthalpy of seawater varies nonlinearly with  
134 temperature and salinity (Fig. 1) and this variation results in non-conservative behavior  
135 under mixing (McDougall (2003), section A.17 of IOC et al. (2010)). The ocean's potential  
136 temperature is subject to internal sources and sinks – it is not conservative.

137 With the development of a Gibbs function for seawater, based on empirical fits to  
138 measurements of known thermodynamic properties (Feistel (2008), IOC et al, 2010), it  
139 became possible to apply a more rigorous theory for quasi-equilibrium thermodynamics  
140 to study heat content problems in the ocean. As a practical matter, calculations can now  
141 be made that allow for an estimate of the magnitude of non-conservative terms in the  
142 ocean circulation. By integrating over water depth this production rate can be expressed  
143 as an equivalent heat flux per unit area.

144 Non-conservation of potential temperature was found to be equivalent to a root  
145 mean square surface heat flux of about  $60 \text{ mW m}^{-2}$  (Graham and McDougall, 2013), and  
146 an average value of  $16 \text{ mW m}^{-2}$  (see below). These numbers can be compared to a  
147 present-day estimated global-warming surface heat flux imbalance of between  
148  $300 \text{ mW m}^{-2}$  and  $470 \text{ mW m}^{-2}$  (Zanna et al., 2019, von Schuckmann et al., 2020). These  
149 equivalent heat fluxes and subsequent similar values are gathered into Table 1 for  
150 reference. In the context of a conceptual ocean model being driven by known heat  
151 fluxes, the presence of the non-conservation of potential temperature causes SST errors  
152 seasonally in the equatorial region of about  $0.5\text{K}$  ( $0.5^{\circ}\text{C}$ ), while the error (in all seasons)  
153 at the outflow of the Amazon is  $1.8\text{K}$  (see section 9 of McDougall, 2003). With different

154 boundary conditions (such as restoring boundary conditions) the error in assuming that  
 155 potential temperature is conservative is split in different proportions, between (a) the  
 156 potential temperature values and (b) the potential temperature fluxes.

157 Unfortunately, no single alternative thermodynamic variable has been found that  
 158 is both independent of pressure, and conservative under mixing. For example, specific  
 159 entropy is produced in the ocean interior when mixing occurs, with the depth-integrated  
 160 production being equivalent to an imbalance in the air-sea heat flux of a root mean  
 161 square value of about  $500 \text{ mW m}^{-2}$  (Graham and McDougall, 2013), while specific  
 162 enthalpy is conservative under mixing at constant pressure, but is intrinsically pressure-  
 163 dependent.

164 However, it was found that a constructed variable, potential enthalpy  
 165 (McDougall, 2003), has a mean non-conservation error in the global ocean of only about  
 166  $0.3 \text{ mW m}^{-2}$  (this is the mean value of an equivalent surface heat flux, equal to the depth  
 167 integrated interior production of potential enthalpy (Graham and McDougall, 2013)).  
 168 The potential enthalpy,  $\tilde{h}^0$ , is the enthalpy of a water parcel after being moved  
 169 adiabatically and at constant salinity to the reference pressure 0 dbar where the  
 170 temperature is equal to the potential temperature,  $\theta$ , of the water parcel:

$$171 \quad \tilde{h}^0(S_A, \theta) = h(S_A, \theta, 0 \text{ dbar}). \quad (1)$$

172 In Eq. (1) the function  $h$  is the specific enthalpy of TEOS-10 (defined as a function of  
 173 Absolute Salinity, in-situ temperature and sea pressure) whereas  $\tilde{h}^0$  is the potential  
 174 enthalpy function and the over-twiddle implies that the temperature input to this  
 175 function is potential temperature,  $\theta$ . By way of comparison, the area-averaged  
 176 geothermal input of heat into the ocean bottom is about  $86 \text{ mW m}^{-2}$ , and the interior  
 177 heating of the ocean due to viscous dissipation, is equivalent to a mean surface heat flux  
 178 of about  $3 \text{ mW m}^{-2}$  (Graham and McDougall, 2013). Thus, potential enthalpy, although  
 179 not a theoretically ideal conservative parameter, can be treated as one for all practical  
 180 purposes in oceanography.

181 Since potential enthalpy is not a widely-understood property, a decision was  
 182 made in the development of TEOS-10 to adopt Conservative Temperature,  $\Theta$ , which has  
 183 units of temperature and is proportional to potential enthalpy:

$$184 \quad \Theta = \tilde{\Theta}(S_A, \theta) = \tilde{h}^0(S_A, \theta) / c_p^0, \quad (2)$$

185 where the proportionality constant  $c_p^0 \equiv 3991.867\,957\,119\,63 \text{ J kg}^{-1} \text{ K}^{-1}$ , was chosen so that  
 186 the average value of Conservative Temperature at the ocean surface matched that of  
 187 potential temperature. Although in hindsight other choices (e.g., with fewer significant  
 188 digits) might have been more useful, this value of  $c_p^0$  is now built into the TEOS-10  
 189 standard.

190 Note that at specific locations in the ocean, in particular at low salinities and high  
 191 temperatures,  $\Theta$  and  $\theta$  can differ by more than  $1^\circ\text{C}$  (Fig. 2); the difference is a strongly  
 192 nonlinear function of temperature and salinity.  $\Theta$  is, by definition, independent of  
 193 adiabatic and isohaline changes in pressure.

194

#### 195 *Why is potential temperature not conservative?*

196 This question is answered in sections A.17 and A.18 of the TEOS-10 Manual (IOC  
 197 et al., 2010) as well as McDougall (2003) and Graham and McDougall (2013). The answer  
 198 is that potential enthalpy referenced to the sea surface pressure,  $h^0$ , which is an (almost  
 199 totally) conservative variable in the real ocean, is not simply a linear function of  
 200 potential temperature,  $\theta$ , and Absolute Salinity,  $S_A$  (and note that both enthalpy and  
 201 entropy are unknown and unknowable up to separate linear functions of Absolute  
 202 Salinity). If potential enthalpy were a linear function of potential temperature and  
 203 Absolute Salinity then the “heat content” per unit mass of seawater could be accurately  
 204 taken to be proportional to potential temperature, and the isobaric specific heat capacity  
 205 at zero sea pressure would be a constant. As an example of the nonlinearity of  $\tilde{h}^0(S_A, \theta)$ ,  
 206 the isobaric specific heat at the sea surface pressure  $c_p(S_A, \theta, 0\text{dbar}) \equiv h_\theta^0$  varies by 6%  
 207 across the full range of temperatures and salinities found in the World Ocean (Fig. 1).  
 208 By way of contrast, the potential enthalpy of an ideal gas is proportional to its potential  
 209 temperature.

210 Another way of treating heat in an ocean model is to continue carrying potential  
 211 temperature as its temperature variable but to (i) use the variable isobaric heat capacity  
 212 at the sea surface to relate the air-sea heat flux to an air-sea flux of potential temperature,  
 213 and (ii) to evaluate the non-conservative source terms of potential temperature and add

214 these source terms to the potential temperature evolution equation during the ocean  
 215 model simulation. This suggestion has been made, for example, by Tailleux (2015).

216 However it is not possible to accurately choose the value of the isobaric heat  
 217 capacity at the sea surface that is needed when  $\theta$  is the model's temperature variable. This  
 218 issue arises because of the unresolved variations in the sea surface salinity (SSS) and SST (for  
 219 example, unresolved rain events that temporarily lower the SSS), together with the nonlinear  
 220 dependence of the isobaric specific heat on salinity and temperature. Hence the air-sea heat  
 221 flux would be systematically mis-estimated. Neither is it possible to accurately estimate the  
 222 non-conservative source terms of  $\theta$ . This problem arises because the source terms are the  
 223 product of a turbulent flux and a mean gradient. In a mesoscale eddy-resolved ocean model  
 224 (or even finer scale) it is not clear how to find the eddy flux of  $\theta$ , as this depends on how the  
 225 averaging is done in space and time. Furthermore, one would need to deal with the  
 226 contributions from source terms that are not expressible in the form of flux convergences  
 227 when analyzing ocean heat transport.

228 We conclude that the idea that ocean models could retain potential temperature  $\theta$  as  
 229 the model's temperature variable, rather than adopt the TEOS-10 recommendation of using  
 230 Conservative Temperature  $\Theta$ , is unworkable because (1) the air-sea heat flux cannot be  
 231 accurately incorporated into the ocean, (2), the non-conservative source terms that appear in  
 232 the  $\theta$  evolution equation cannot be estimated accurately, and (3) the ocean section-  
 233 integrated heat fluxes cannot be accurately calculated.

234

### 235 *How conservative is Conservative Temperature?*

236 This question is addressed in McDougall (2003) as well as in section A.18 of the  
 237 TEOS-10 Manual (IOC et al., 2010) and in Graham and McDougall (2013). The first step  
 238 in addressing the non-conservation of  $\Theta$  is to find a thermophysical variable that is  
 239 conserved when fluid parcels mix. McDougall (2003) and Graham and McDougall  
 240 (2013) showed that when fluid parcels are brought together adiabatically and at constant  
 241 salinity to mix at pressure  $p^m$ , it is the potential enthalpy  $h^m$  referenced to the pressure  
 242  $p^m$  of a mixing event that is conserved, apart from the dissipation of kinetic energy,  $\varepsilon$ .



243 From this knowledge they constructed the evolution equations for Conservative  
 244 Temperature as well as for potential temperature and entropy.

245 By contrast, Tailleux (2010) and Tailleux (2015) assumed that it was the Total  
 246 Energy, being the sum of internal energy, kinetic energy and the geopotential, that is  
 247 conserved when fluid parcels mix in the ocean. However, as shown by McDougall,  
 248 Church and Jackett (2003), the  $-\nabla \cdot (P\mathbf{u})$  term on the right-hand side of the evolution  
 249 equation for Total Energy is non-zero when integrated over the mixing region, so that  
 250 Total Energy is not a conservative variable. Tailleux (2010, 2015) also ignored this non-  
 251 conservative term,  $-\nabla \cdot (P\mathbf{u})$ , so that they actually arrived at the correct evolution  
 252 equations for  $\Theta$ ,  $\theta$  and  $\eta$  (for example, Eqn. (B.7) of Tailleux (2010) and Eqn. (B10) of  
 253 Graham and McDougall (2013) are identical). However, these equations are written in  
 254 terms of the molecular fluxes of heat and salt, and it is not possible to use these  
 255 expressions to evaluate the non-conservation of  $\Theta$ ,  $\theta$  and  $\eta$  in a turbulently mixed  
 256 ocean.

257 While enthalpy is conserved when mixing occurs at constant pressure, it does not  
 258 possess the “potential” property, but rather, an adiabatic and isohaline change in  
 259 pressure causes a change in enthalpy according to  $\hat{h}_p = v$ , where  $v$  is the specific  
 260 volume. This property is illustrated in Fig. 3 where it is seen that for an adiabatic and  
 261 isohaline increase of pressure of 1000dbar, the increase in enthalpy is the same as that  
 262 caused by an increase in Conservative Temperature of more than 2.4°C. If enthalpy  
 263 variations at constant pressure were a linear function of Absolute Salinity and  
 264 Conservative Temperature, the contours in Fig. 3 would be parallel equidistant straight  
 265 lines, and Conservative Temperature would be totally conservative. Since this is not the  
 266 case, this figure illustrates the (small) non-conservation of Conservative Temperature.

267

### 268 *Seawater Salinity*

269 To a degree of approximation which is useful for many purposes, the dissolved  
 270 matter in seawater (“sea salt”) can be treated as a material of uniform composition,  
 271 whose absolute salinity (i.e. the grams of solute per kilogram of seawater) changes only  
 272 due to the addition and removal of freshwater through rain, evaporation, and river

273 inflow. This property is because the processes that govern the addition and removal of  
274 the constituents of sea salt have extremely long time scales, relative to those that affect  
275 the pure water component of seawater. We can thus treat the total ocean salt content as  
276 approximately constant, while subject to spatially and temporally varying boundary  
277 fluxes of fresh water that give rise to salinity gradients.

278 The utility of this definition of uniform composition of sea salt lies in its  
279 conceptual simplicity, well suited to theoretical and numerical ocean modelling at time  
280 scales of up to 100s of years. However, to the demanding degree required for observing  
281 and understanding deep ocean pressure gradients, sea salt is neither uniform in  
282 composition, nor is it a conserved variable, nor can its absolute amount be measured  
283 precisely in practice. The repeatable precision of various technologies used to estimate  
284 salinity can be as small as 0.002 g/kg, but the non-ideal nature of seawater means that  
285 these estimates can be different by as much as 0.025 g/kg relative to the true Absolute  
286 Salinity in the open ocean, and as much 0.1 g/kg in coastal areas (Pawlowicz, 2015).

287 The most important interior source and sink factors governing changes in the  
288 composition of sea salt are biogeochemical processes that govern the biological uptake of  
289 dissolved nutrients, calcium, and carbon in the upper ocean, and the remineralization of  
290 these substances from sinking particles at depth. At present it is thought that changes  
291 resulting from hydrothermal vent activity, fractionation from sea ice formation, and  
292 through multi-component molecular diffusion processes are of local importance only,  
293 but little work has been done to quantify this.

294 In order to address this problem, TEOS-10 defines a Reference Composition of  
295 seawater, and a number of slightly different salinity variables that are necessary for  
296 different purposes to account for the variable composition of sea salt. The TEOS-10  
297 Absolute Salinity,  $S_A$ , is the absolute salinity of Reference Composition Seawater of a  
298 measured density (note that capitalization of variable names denotes a precise definition  
299 in TEOS-10). It is the only salinity variable that can be properly used in calculations of  
300 density using the TEOS-10 Gibbs function.

301 Preformed Salinity,  $S_*$ , is the salinity of a seawater parcel with the effects of  
302 biogeochemical processes removed, somewhat analogous to a chlorinity-based salinity

303 estimate. It is thus a conservative tracer of seawater, suitable for modelling purposes,  
 304 but neglects the spatially-variable small portion of sea salt involved in biogeochemical  
 305 processes that is required for the most accurate density estimates. Since the original  
 306 measurements of specific volume to which both EOS-80 and TEOS-10 were fitted were  
 307 made on samples of Standard Seawater with composition close to Reference  
 308 Composition, the Reference Salinity of these samples were also the same as Preformed  
 309 Salinity.

310 Ocean observational databases contain a completely different variable; Practical  
 311 Salinity. This variable, which predates TEOS-10, is essentially based on a measure of the  
 312 electrical conductance of seawater, normalized to conditions of fixed temperature and  
 313 pressure by empirical correlation equations, between the ranges of 2 and 42 PSS-78 and  
 314 scaled so that ocean salinity measurements that have been made through a variety of  
 315 technologies over the past 120 years are numerically comparable. Practical Salinity  
 316 measurement technologies involve a certified reference material called IAPSO Standard  
 317 Seawater, which for our purposes can be considered the best available artifact  
 318 representing seawater of Reference Composition.

319 Practical Salinity was not designed for numerical modelling purposes and does not  
 320 accurately represent the mass fraction of dissolved matter. We can link Practical  
 321 Salinity,  $S_p$ , to the Absolute Salinity of Reference Composition seawater (so-called  
 322 Reference Salinity,  $S_R$ ) using a fixed scale factor,  $u_{ps}$ , so that

$$323 \quad S_R = u_{ps} S_p \quad \text{where} \quad u_{ps} \equiv (35.165\,04/35) \text{ g kg}^{-1}. \quad (3)$$

324 Conversions to and between the other “salinity” definitions, however, involve  
 325 knowledge about spatial and temporal variations in seawater composition. Fortunately,  
 326 the largest component of these changes occurs in a set of constituents involved in  
 327 biogeochemical processes, whose co-variation is known to be strongly correlated. Thus  
 328 the Absolute Salinity of real seawater can be determined globally to useful accuracy  
 329 from the Reference Salinity by the addition of a single parameter, the so-called Absolute  
 330 Salinity Anomaly,  $\delta S_A$ ,

$$331 \quad S_A = S_R + \delta S_A, \quad (4)$$

332 which has been tabulated in a global atlas for the current ocean (McDougall et al., 2012),  
 333 and is estimated in coastal areas by considering the effects of river salts (Pawlowicz,  
 334 2015). It can also be determined from measurements of either density or of carbon and  
 335 nutrients (IOC et al., 2010). For purposes of numerical ocean modelling, the Absolute  
 336 Salinity Anomaly could in theory be obtained by separately tracking the carbon cycle  
 337 and nutrients, and applying known correction factors, but we are not aware of any  
 338 attempts to do so.

339 Chemical modelling (Pawlowicz (2010), Wright et al. (2011), Pawlowicz et al.  
 340 (2012)) suggests the approximate relation

$$341 \quad S_A - S_* \approx 1.35 \delta S_A \equiv 1.35(S_A - S_R), \quad (5)$$

342 and these relationships are schematically illustrated in Fig. 4. The magnitude of the  
 343 Absolute Salinity Anomaly is around -.005 to +0.025 g/kg in the open ocean, relative to a  
 344 mean Absolute Salinity of about 35 g/kg. The correction it implies may be important  
 345 when initializing models, or comparing them with observations, but its major effect is  
 346 likely in producing biases in calculated isobaric density gradients.

347

### 348 *Seawater density*

349 The density of seawater is the most important thermodynamic property affecting  
 350 oceanic motions, since its spatial changes (along with changes to the sea-surface height)  
 351 give rise to pressure gradients which are the primary driving force for currents within  
 352 the ocean interior through the hydrostatic relation. The “traditional” equation of state is  
 353 known as EOS-80 (UNESCO, 1981), and is standardized as a function of Practical  
 354 Salinity and in-situ temperature,  $\rho = \rho(S_p, t, p)$ , which has 41 numerical terms. An  
 355 additional equation (the adiabatic lapse rate) is required for conversion of temperature  
 356 to potential temperature. However, for ocean models, the equation of state is usually  
 357 taken to be the 41-term expression written in terms of potential temperature,  
 358  $\rho = \tilde{\rho}(S_p, \theta, p)$ , of Jackett and McDougall (1995), where the over-twiddle indicates that  
 359 this rational function fit was made with Practical Salinity  $S_p$  and potential temperature  
 360  $\theta$  as the input salinity and temperature variables.

361 The current standard for describing the thermodynamic properties of seawater,  
 362 known as TEOS-10, provides an equation of state,  $v = 1/\rho = v(S_A, t, p)$ , in the form of a  
 363 function which involves 72 coefficients (IOC et al., 2010) and is an analytical pressure  
 364 derivative of the TEOS-10 Gibbs function. However, for ocean models using TEOS-10  
 365 the equation of state used is one of those in Roquet et al. (2015); the 55-term equation of  
 366 state,  $\rho = \hat{\rho}(S_A, \Theta, z)$ , used by Boussinesq models and the 75-term form in terms of  
 367 specific volume,  $v = \hat{v}(S_A, \Theta, p)$ , used by non-Boussinesq ocean models.

368 In this paper we will not concentrate on the distinction between Boussinesq and  
 369 non-Boussinesq ocean models, and henceforth we will take the third input to the  
 370 equation of state to be pressure, even though for a Boussinesq model it is in fact a scaled  
 371 version of depth as per the energetic arguments of Young (2010). By the same token, we  
 372 will cast the discussion in terms of the *in situ* density, even though the non-Boussinesq  
 373 models have as their equation of state a polynomial for the specific volume,  $v = 1/\rho$ .

374 For seawater of Reference Composition, both the TEOS-10 and EOS-80 fits  
 375  $\rho = \hat{\rho}(S_A, \Theta, p)$  and  $\rho = \tilde{\rho}(S_p, \theta, p)$  are almost equally accurate (see section A.5 of IOC et  
 376 al. (2010), and in particular, note the comparison between Figures A.5.1 and A.5.2  
 377 therein). That is, if we set  $\delta S_A = 0$  and use Eqn. (3) to relate Practical and Reference  
 378 Salinities (which in this case are the same as Preformed Salinities), the numerical density  
 379 values of *in situ* density calculated using EOS-80 are not significantly different to those  
 380 using TEOS-10.

381 This being the case, we can see from section A.5 and A.20 of the TEOS-10 Manual  
 382 (IOC et al. (2010)) that 58% of the data deeper than 1000 dbar in the World Ocean would  
 383 have the thermal wind misestimated by  $\sim 2.7\%$  due to ignoring the difference between  
 384 Absolute and Reference Salinities. No ocean model has addressed this deficiency to  
 385 date, but McCarthy et al. (2015) studied the influence of using Absolute Salinity versus  
 386 Reference Salinity in calculating the overturning circulation in the North Atlantic. They  
 387 found that the overturning streamfunction changed by 0.7Sv at a depth of 2700m,  
 388 relative to a mean value at this depth of about 7 Sv, i.e. a 10% effect. Because we argue  
 389 that the salinity variable in ocean models is best interpreted as being Preformed Salinity,  
 390  $S_*$ , the neglect of the distinction between Preformed and Absolute Salinities in ocean

391 models means that they mis-estimate the overturning streamfunction by 1.35 (see Figure  
392 4) times  $0.7\text{Sv}$ , namely  $\sim 1\text{Sv}$ , i.e. a 13.5% effect.

393

#### 394 *Air-sea heat fluxes*

395     Sensible, latent and long-wave radiative fluxes are affected by near-surface  
396 turbulence and are usually calculated using bulk formulae involving air and sea  
397 surface water temperatures (the air and sea *in situ* temperatures), as well as other  
398 parameters (e.g., the latent heat involves the isobaric evaporation enthalpy, commonly  
399 called the latent heat of evaporation, which is actually a weak function of temperature  
400 and salinity; see Eqn. 6.28 of Feistel et al. (2010) and Eqn. (3.39.7) of IOC et al. (2010)).  
401 The total air-sea heat flux,  $Q$ , is then translated into a water temperature change by  
402 dividing by a heat capacity  $c_p^0$ , which has always been taken to be constant in  
403 numerical models (Griffies et al., 2016). Although this method is appropriate for  
404 Conservative Temperature, CT, (assuming that the TEOS-10 value is used for  $c_p^0$ ), it is  
405 not appropriate when potential temperature is being considered. The flux of potential  
406 temperature into the surface of the ocean should be  $Q$  divided by  $c_p(S_*, \theta, 0)$ . The use  
407 of a constant specific heat capacity, in association with the interpretation of the  
408 ocean's temperature variable as being potential temperature, means that the ocean has  
409 received a different amount of heat than the atmosphere actually delivers to the ocean,  
410 and this issue will be explored in section 3.

411     When precipitation ( $P$ ) occurs at the sea surface, this addition of freshwater  
412 brings with it the associated potential enthalpy  $h(S_A=0, t, 0\text{dbar})$  per unit mass of  
413 freshwater, where  $t$  is the *in situ* temperature of the rain drops as they arrive at the sea  
414 surface. The temperature at which rain enters the ocean is not yet treated consistently in  
415 coupled models, and section K1.6 of Griffies et al. (2016) suggests that this effect could  
416 be equivalent to an area-averaged extra air-sea heat flux of between  $-150\text{mWm}^{-2}$   
417 and  $-300\text{mWm}^{-2}$ , representing a heat loss for the ocean.

418

419

## 420 *Numerical ocean models*

421 In deciding how to numerically model the ocean, an explicit choice must be made  
 422 about the equation of state, and one would think that this choice would have  
 423 implications about the precise meaning of the temperature and salinity variables in the  
 424 model, which we will call  $T_{\text{model}}$  and  $S_{\text{model}}$  respectively. We can divide ocean models  
 425 into two general classes, EOS-80 models and TEOS-10 models:

426

### 427 EOS-80 models

428 One class of CMIP ocean model is based around EOS-80, and these models have the  
 429 following characteristics:

- 430 1. The model's equation of state,  $\rho = \tilde{\rho}(S_p, \theta, p)$ , expects to have Practical Salinity  
 431 and potential temperature as the salinity and temperature input parameters.
- 432 2.  $T_{\text{model}}$  is advected and diffused in the ocean interior in a conservative manner; i.e.,  
 433 its evolution at a point in space is determined by the convergence of advective  
 434 fluxes plus parameterized subgrid scale diffusive and skew diffusive fluxes.
- 435 3.  $S_{\text{model}}$  is advected and diffused in the ocean interior in a conservative manner as  
 436 for  $T_{\text{model}}$ .
- 437 4. The air-sea heat flux is delivered to/from the ocean using a constant isobaric  
 438 specific heat,  $c_p^0$ , to convert the air-sea heat flux into a surface flux of  $T_{\text{model}}$ . [An  
 439 EOS-80 based model's value of  $c_p^0$  is generally only slightly different to the  
 440 TEOS-10 value.]
- 441 5.  $T_{\text{model}}$  is initialized from an atlas of values of potential temperature, and  $S_{\text{model}}$  is  
 442 initialized with values of Practical Salinity.

443 At first glance, it seems reasonable to assume that  $T_{\text{model}}$  is potential temperature, and  
 444  $S_{\text{model}}$  is Practical Salinity. However, these assumptions imply that theoretical errors  
 445 arising from items 2 and 3 and 4 are ignored (since neither potential temperature nor  
 446 Practical Salinity are conservative variables). In this paper we show that these  
 447 interpretations of the model's temperature and salinity variables are not as accurate as  
 448 our proposed alternative interpretations.

449

450 TEOS-10 models

451 Other ocean models have begun to implement TEOS-10 features. These models  
 452 generally have the following characteristics.

- 453 1. The model's equation of state,  $\rho = \hat{\rho}(S_A, \Theta, p)$ , expects to have Absolute Salinity  
 454 and Conservative Temperature as its salinity and temperature input parameters.
- 455 2.  $T_{\text{model}}$  is advected and diffused in the ocean interior in a conservative manner.
- 456 3.  $S_{\text{model}}$  is advected and diffused in the ocean interior in a conservative manner.
- 457 4. At each time step of the model, the value of potential temperature at the sea  
 458 surface (i.e. SST) is calculated from the  $T_{\text{model}}$  (which is assumed to be  
 459 Conservative Temperature) and this value of SST is used to interact with the  
 460 atmosphere via bulk flux formulae.
- 461 5. The air-sea heat flux is delivered to/from the ocean using the TEOS-10 constant  
 462 isobaric specific heat,  $c_p^0$ , to convert the air-sea heat flux into a surface flux of  
 463  $T_{\text{model}}$ .
- 464 6.  $T_{\text{model}}$  is initialized from an atlas of values of Conservative Temperature, and  
 465  $S_{\text{model}}$  is initialized with values of one of Absolute Salinity, Reference Salinity or  
 466 Preformed Salinity.

467 Implicitly, it has then been assumed that  $T_{\text{model}}$  is a Conservative Temperature, and  $S_{\text{model}}$   
 468 is Absolute Salinity.

469 There is one CMIP6 ocean model that we are aware of, ACCESS-CM2 (Australian  
 470 Community Climate and Earth System Simulator, Bi et al. 2013), whose equation of state  
 471 is written in terms of Conservative Temperature, but the salinity argument in the  
 472 equation of state is Practical Salinity. The salinity in this model is initialized with atlas  
 473 values of Practical Salinity.

474 From the above, it is clear that there are small but significant theoretical  
 475 incompatibilities between different models, and between models and the observed  
 476 ocean. These issues become apparent when dealing with the technicalities of  
 477 intercomparisons, and various choices must be made. We now consider the implications  
 478 of these different choices and provide recommendations for best practices.

479



### 480 3. The Interpretation of salinity in ocean models

481 Note that the samples whose measured specific volumes were incorporated into  
 482 both the EOS-80 and TEOS-10 equations of state were of Standard Seawater whose  
 483 composition is close to Reference Composition. Consequently, the EOS-80 and TEOS-10  
 484 equations of state were constructed with Preformed Salinity,  $S_*$  (or, in the case of EOS-  
 485 80 models,  $S_*/u_{\text{PS}}$ ), as their salinity arguments, not Reference Salinity. These same  
 486 algorithms give accurate values of specific volume for seawater samples that are not of  
 487 Reference Composition so long as the salinity argument is Absolute Salinity (as opposed  
 488 to Reference Salinity or Preformed Salinity).

489 For an ocean model that has no non-conservative interior source terms affecting  
 490 the evolution of its salinity variable, and that is initialized at the sea surface with  
 491 Preformed Salinity, the only interpretation for the model's salinity variable is Preformed  
 492 Salinity, and the use of the TEOS-10 equation of state will then yield the correct specific  
 493 volume. Furthermore, whether the model is initialized with values of Absolute Salinity,  
 494 Reference Salinity or Preformed Salinity, these initial salinity values are nearly identical  
 495 in the upper ocean, and any differences between the three initial conditions in the  
 496 deeper ocean would be largely diffused away within the long spin-up period. That is, in  
 497 the absence of the non-conservative biogeochemical source terms that would be needed  
 498 to model Absolute Salinity and to force it away from being conservative (or the smaller  
 499 source terms that would be needed to maintain Reference Salinity), the model's salinity  
 500 variable will drift towards being Preformed Salinity. Hence, we conclude that, after the  
 501 long spin-up phase, the salinity variable of a TEOS-10 based ocean model is accurately  
 502 interpreted as being Preformed Salinity  $S_*$ , irrespective of whether the model was  
 503 initialized with values of Absolute Salinity, Reference Salinity or Preformed Salinity.

504 Likewise, the prognostic salinity variable after a long spin-up period of an EOS-  
 505 80 based model is most accurately interpreted as being Preformed Salinity divided by  
 506  $u_{\text{PS}} \equiv (35.165\ 04/35) \text{ g kg}^{-1}$ ,  $S_*/u_{\text{PS}}$ .

507 We clearly need more estimates of the magnitude of the dynamic effects of the  
 508 variable seawater composition, but for now we might take a change in 1 Sv in the  
 509 meridional transport of deep water masses in each ocean basin (based on the Atlantic

510 work of McCarthy et al., 2015) as an indication of the magnitude of the effect of  
 511 neglecting the effects of biogeochemistry on salinity. At this stage of model  
 512 development, since all models are equally deficient in their thermophysical treatment of  
 513 salinity, at least this aspect does not present a problem as far as making comparisons  
 514 between CMIP models.

515

#### 516 **4. Model Heat Flux Calculations**

517 From the details described above, both types of numerical ocean models suffer from  
 518 some internal contradictions with thermodynamical best practice. For example, for the  
 519 EOS-80 based models, if  $T_{\text{model}}$  is assumed to be potential temperature, the use of EOS-80  
 520 is correct for density calculations but the use of conservative equations for  $T_{\text{model}}$  ignores  
 521 the non-conservative production of potential temperature. The use of a constant heat  
 522 capacity is also in error if  $T_{\text{model}}$  is interpreted as potential temperature. Conservative  
 523 equations are, however, appropriate for Conservative Temperature. In addition, if  $S_{\text{model}}$   
 524 is assumed to be either Practical Salinity or Absolute Salinity, then the use of  
 525 conservative equations ignores the changes in salinity that arise from biogeochemical  
 526 processes.

527 One use for these models is to calculate heat budgets and heat fluxes – both at the  
 528 surface and between latitudinal bands, and inherent to CMIP is the idea that these  
 529 different models should be intercompared. The question of how this intercomparison  
 530 should be done, however, was not clearly addressed in Griffies et al. (2016). Here we  
 531 begin the discussion by considering two different options for interpreting  $T_{\text{model}}$  in EOS-  
 532 80 ocean models.

533

#### 534 **4.1 Option 1: interpreting the EOS-80 model's temperature as being potential**

##### 535 *temperature*

536 Under this option the model's temperature variable  $T_{\text{model}}$  is treated as being potential  
 537 temperature  $\theta$ ; this is the prevailing interpretation to date. With this interpretation of  
 538  $T_{\text{model}}$  one wonders whether Conservative Temperature  $\Theta$  should be calculated from the  
 539 model's (assumed) potential temperature before calculating (i) the global Ocean Heat

540 Content as the volume integral of  $\rho c_p^0 \Theta$ , and (ii) the advective meridional heat transport  
 541 as the area integral of  $\rho c_p^0 \Theta v$  at constant latitude, where  $v$  is the northward velocity.  
 542 This question was not clearly addressed in Griffies et al. (2016), and here we emphasize  
 543 one of the main conclusions of the present paper, namely that ocean heat content and  
 544 meridional heat transports should be calculated using the model's prognostic  
 545 temperature variable. Any subsequent conversion from one temperature variable to  
 546 another (such as potential to Conservative) in order to calculate heat content and heat  
 547 transport is incorrect and confusing, and should not be attempted.

548

#### 549 *4.1.1 Issues with the potential temperature interpretation*

550 There are several thermodynamic inconsistencies that arise from option 1. First,  
 551 the ocean model has assumed in its spin-up phase (for perhaps a millennium) that  $T_{\text{model}}$   
 552 is conservative, so during the whole spin-up phase and beyond, the contribution of the  
 553 known non-conservative interior source terms of potential temperature have been  
 554 absent, and hence the model's temperature variable has not responded to these absent  
 555 source terms and so this temperature field cannot be potential temperature. Also, since  
 556 the temperature field of the model is not potential temperature (because of these absent  
 557 source terms) the velocity field of the model will also not be forced correctly due to  
 558 errors in the density field which in turn affect the pressure force.

559 The second inconsistent aspect of option 1 is that the air-sea flux of heat is  
 560 ingested into the ocean model, both during the spin-up stage and during the transient  
 561 response phase, as though the model's temperature variable is proportional to potential  
 562 enthalpy. For example, consider some time during the year at a particular location  
 563 where the sea surface is fresh (a river outflow, or melted ice). During this time, any heat  
 564 that the atmosphere loses or gains should have affected the potential temperature of the  
 565 upper layers of the ocean using a specific heat that is 6% larger than  $c_p^0$  (see Figure 1).  
 566 So, if the ocean model's temperature variable is interpreted as being potential  
 567 temperature, a 6% error is made in the heat flux that is exchanged with the atmosphere  
 568 during these periods/locations. That is, the changes in the ocean model's (assumed)  
 569 potential temperature caused by the air-sea heat flux will be exaggerated where and

570 when the sea surface salinity is fresh. This 6% flux error is not corrected by  
 571 subsequently calculating Conservative Temperature from potential temperature; for  
 572 example, these temperatures are the same at low temperature and salinity (see Figure 2),  
 573 and yet at low values of salinity, the specific heat is 6% larger than  $c_p^0$ .

574 This second inconsistent aspect of option 1 can be restated as follows. The  
 575 adoption of potential temperature as the model's temperature variable means that there  
 576 is a discontinuity in the heat flux of the coupled air-sea system right at the sea surface;  
 577 for every Joule of heat (i.e. potential enthalpy) that the atmosphere gives to the ocean,  
 578 under this Option 1 interpretation, up to 6% too much heat arrives in the ocean over  
 579 relatively fresh waters. In this way, the adoption of potential temperature as the model  
 580 temperature variable ensures that the coupled ocean atmosphere system will not  
 581 conserve heat. Rather, there appear to be non-conservative sources and sinks of heat  
 582 right at the sea surface where heat is unphysically manufactured or destroyed.

583 The third inconsistent aspect is a direct consequence of the second; namely that if  
 584 one is tempted to post-calculate Conservative Temperature  $\Theta$  from the model's  
 585 (assumed) values of potential temperature, the rate of change of the calculated ocean  
 586 heat content as the volume integral of  $\rho c_p^0 \Theta$  would no longer be accurately related to the  
 587 heat that the atmosphere exchanged with the ocean. Neither would the area integral  
 588 between latitude bands of the air-sea heat flux be exactly equal to the difference between  
 589 the calculated oceanic meridional heat transports that cross those latitudes. Rather,  
 590 during the running of the model the heat that was lost from the atmosphere actually  
 591 shows up in the ocean as the volume integral of the model's prognostic temperature  
 592 variable. We agree with Appendix D3.3 of Griffies et al. (2016) and strongly recommend  
 593 that Conservative Temperature is not calculated *a posteriori* in order to evaluate heat  
 594 content and heat fluxes in these EOS-80 based models.

595

#### 596 4.1.2 Quantifying the air-sea flux imbalance

597 Here we quantify the air-sea flux errors involved with assuming that  $T_{\text{model}}$  of  
 598 EOS-80 models is potential temperature. These EOS-80 based models calculate the air-  
 599 sea flux of their model's temperature as the air-sea heat flux,  $Q$ , divided by  $c_p^0$ .

600 However, since the isobaric specific heat capacity of seawater at 0 dbar is  $c_p(S_*,\theta,0)$ , the  
 601 flux of potential temperature into the surface of the ocean should be  $Q$  divided by  
 602  $c_p(S_*,\theta,0)$ . So, if the model's temperature variable is interpreted as being potential  
 603 temperature, the EOS-80 model has a flux of potential temperature entering the ocean  
 604 that is too large by the difference between these fluxes, namely by  $Q/c_p^0$  minus  
 605  $Q/c_p(S_*,\theta,0)$ . This means that the ocean has received a different amount of heat than the  
 606 atmosphere actually delivers to the ocean, with the difference,  $\Delta Q$ , being  $c_p(S_*,\theta,0)$   
 607 times the difference in the surface fluxes of potential temperature, namely (for the last  
 608 part of this equation, see Eqn. (A.12.3a) of IOC et al., 2010)

$$609 \quad \Delta Q = Q \left( \frac{c_p(S_*,\theta,0)}{c_p^0} - 1 \right) = Q(\tilde{\Theta}_\theta - 1). \quad (6)$$

610 We plot this quantity from the pre-industrial control run of ACCESS-CM2 in  
 611 Figure 5c and show it as a cell area-weighted histogram in Figure 5e (note that while  
 612 these plots apply to EOS-80 based ocean models, to generate these plots we have  
 613 actually used data from ACCESS-CM2 which is a mostly TEOS-10 compliant model).  
 614 The calculation takes into account the penetration of shortwave radiation into the ocean  
 615 but is performed using monthly-averages of the thermodynamics quantities. The  
 616 temperatures and salinities at which the radiative flux divergences occur are taken into  
 617 account in this calculation. However, the result is little changed if the sea surface  
 618 temperatures and salinities are used with the radiative flux divergence assumed to take  
 619 place at the sea surface. Results from similar calculations performed using monthly and  
 620 daily-averaged quantities in ACCESS-OM2 (Kiss et al. 2020) ocean-only model  
 621 simulations were similar, suggesting that correlations between sub-monthly variations  
 622 are not significant (at least in these relatively coarse-resolution models).

623  $\Delta Q$  has an area-weighted mean value of  $16 \text{ mW m}^{-2}$  and we know that this  
 624 represents the net surface flux of potential temperature required to balance the volume  
 625 integrated non-conservation of potential temperature in the ocean's interior (Tailleux  
 626 (2015)). To put this value in context,  $16 \text{ mW m}^{-2}$  corresponds to 5% of the observed trend  
 627 of  $300 \text{ mW m}^{-2}$  in the global ocean heat content from 1955-2017 (Zanna et al. 2019). In  
 628 addition to this mean value of  $\Delta Q$ , we see from Figure 5c that there are small regions

629 such as the equatorial Pacific and the western north Pacific where  $\Delta Q$  is as large as the  
 630 area-averaged heat flux,  $300 \text{ mW m}^{-2}$ , that the ocean has received since 1955. These local  
 631 anomalies of air-sea flux, if they existed, would drive local variations in temperature.  
 632 However, these  $\Delta Q$  values do not represent real heat fluxes. Rather they represent the  
 633 error in the air-sea heat flux that we make if we insist that the temperature variable in an  
 634 EOS-80 based ocean model is potential temperature, with the ocean receiving a surface  
 635 heat flux that is larger by  $\Delta Q$  than the atmosphere delivers to the ocean. Figure 6 shows  
 636 the zonal integration of  $\Delta Q$ , in units of W per degree of latitude.

637 Figure 5e shows that, with  $T_{\text{model}}$  being interpreted as potential temperature, 5%  
 638 of the surface area of the ocean needs a surface heat flux that is more than  $135 \text{ mW m}^{-2}$   
 639 different to what the atmosphere gives to/from the ocean. This regional variation of  $\Delta Q$   
 640 of approximately  $\pm 100 \text{ mW m}^{-2}$  is consistent with the regional variations in air-sea flux of  
 641 potential temperature found by Graham and McDougall (2013) that is needed to balance  
 642 the depth-integrated non-conservation of potential temperature as a function of latitude  
 643 and longitude. Figures 5d,f show that much of this spread is due to the variation of the  
 644 isobaric specific heat capacity on salinity, with the remainder due to the variation of this  
 645 heat capacity with temperature. We note that if this analysis were performed with a  
 646 model that resolved individual rain showers and the associated freshwater lenses on the  
 647 ocean surface, then these episodes of very fresh water at the sea surface would be  
 648 expected to increase the calculated values of  $\Delta Q$ . Interestingly, by way of contrast, it is  
 649 the variation of the isobaric heat capacity with temperature that dominates (by a factor  
 650 of four) the contribution of this heat capacity variation to the area mean of  $\Delta Q$  (with the  
 651 contribution of salinity,  $\Delta Q_s$ , in Figure. 5d, leading to an area mean of  $4 \text{ mW m}^{-2}$ ), as  
 652 originally found by Tailleux (2015).

653 While a heat flux error of  $\pm 100 \text{ mW m}^{-2}$  is not large, it also not trivially small, and  
 654 it seems advisable to respect these fundamental thermodynamic aspects of the coupled  
 655 Earth system. We will see that this  $\pm 100 \text{ mW m}^{-2}$  issue is simply avoided by realizing  
 656 that the temperature variable in these EOS-80 models is not potential temperature.

657 In Appendix A we enquire whether the way that EOS-80 models treat their fluid  
 658 might be made to be thermodynamically correct for a fluid other than seawater. We find

659 that it is possible to construct such a thermodynamic definition of a fluid with the aim  
660 that its treatment in EOS-80 models is consistent with the laws of thermodynamics. This  
661 fluid has the same specific volume as seawater for given values of salinity, potential  
662 temperature and pressure, but it has different expressions for both enthalpy and  
663 entropy. This fluid also has a different adiabatic lapse rate and therefore a different  
664 relationship between *in situ* and potential temperatures. However, this exercise in  
665 thermodynamic abstraction does not alter the fact that, as a model of the real ocean, and  
666 with the temperature variable being interpreted as being potential temperature, the  
667 EOS-80 models have  $\Delta Q$  more heat arriving in the ocean than leaves the atmosphere.

668         Since CMIP6 is centrally concerned with how the planet warms, it is advisable to  
669 adopt a framework where heat fluxes and their consequences are respected. That is, we  
670 regard it as imperative to avoid non-conservative sources of heat at the sea surface. It is  
671 the insistence that the temperature variable in EOS-80 based models is potential  
672 temperature that implies that the ocean receives a heat flux from the atmosphere that is  
673 larger by  $\Delta Q$  than what the atmosphere actually exchanges with the ocean. Since there  
674 are some areas of the ocean surface where  $\Delta Q$  is as large as the mean rate of global  
675 warming, Option 1 is not supportable. This situation motivates Option 2 where we  
676 change the interpretation of the model's temperature variable from being potential  
677 temperature to Conservative Temperature even when using EOS-80.

678

#### 679 **4.2 Option 2: interpreting the EOS-80 model's temperature as being Conservative**

##### 680 **Temperature**

681 Under this option the ocean model's temperature variable is taken to be Conservative  
682 Temperature  $\Theta$ . The air-sea flux of potential enthalpy is then correctly ingested into the  
683 ocean model using the fixed specific heat  $c_p^0$ , and the mixing processes in the model  
684 correctly conserve Conservative Temperature. Hence the second, fourth and fifth items  
685 listed in section 2 are handled correctly, except for the following caveat. In the coupled  
686 model, the bulk formulae that set the air-sea heat flux at each time step use the  
687 uppermost model temperature as the sea surface temperature as input. So with the  
688 Option 2 interpretation of the model's temperature variable as being Conservative

689 Temperature, these bulk formulae are not being fed the SST (which at the sea surface is  
 690 equal to the potential temperature  $\theta$ ). The difference between these temperatures is  
 691  $\Theta - \theta$ , which is the negative of what we plot in Figure 2. This is a caveat with this  
 692 Option 2 interpretation, namely that the bulk formula that the model uses to determine  
 693 the air-sea flux at each time step is a little bit different to what was intended when the  
 694 parameters of the bulk formulae were chosen. This is a caveat regarding what was  
 695 intended by the coupled modeler, rather than what the coupled model experienced.  
 696 That is, with this Option 2 interpretation, the air-sea heat flux, while being a little bit  
 697 different than what might have been intended, does arrive in the ocean properly; there is  
 698 no non-conservative production or destruction of heat at the air-sea boundary as there is  
 699 in Option 1.

700 Regarding the remaining two items involving temperature listed in section 2, we  
 701 can dismiss the fifth item, since any small difference in the initial values, set at the  
 702 beginning of the lengthy spin-up period, between potential temperature and  
 703 Conservative Temperature will be irrelevant after the long spin-up integration.

704 This then leaves the first point, namely that the model used the equation of state  
 705 that expects potential temperature as its temperature input,  $\tilde{\rho}(S_*/u_{ps}, \theta, p)$ , but under  
 706 this Option 2 we are interpreting the model's temperature variable as being  
 707 Conservative Temperature. In the remainder of this section we address the magnitude  
 708 of this effect, namely, the use of  $\tilde{\rho}(S_*/u_{ps}, \Theta, p)$  versus the correct density  $\tilde{\rho}(S_*/u_{ps}, \theta, p)$   
 709 which is almost the same as  $\hat{\rho}(S_*, \Theta, p)$ . Note, as discussed in section 3 above, the  
 710 salinity argument of the TEOS-10 equation of state is taken to be  $S_*$  while that of the  
 711 EOS-80 equation of state is taken to be  $S_*/u_{ps}$ . These salinity variables are simply  
 712 proportional to each other, and they have the same influence in both equations of state.

713 Under this Option 2 we are interpreting the model's temperature variable as  
 714 being Conservative Temperature, and so the density value that the model calculates  
 715 from its equation of state is deemed to be  $\tilde{\rho}(S_*/u_{ps}, \Theta, p)$  whereas the density should be  
 716 evaluated as  $\hat{\rho}(S_*, \Theta, p)$  where we remind ourselves that the hat over the *in situ* density  
 717 function indicates that this is the TEOS-10 equation of state, written with Conservative  
 718 Temperature as its temperature input. To be clear, under EOS-80 and under TEOS-10



719 the *in situ* density of seawater of Reference Composition has been expressed by two  
720 different expressions,

$$721 \quad \rho = \tilde{\rho}(S_*/u_{\text{PS}}, \theta, p) = \hat{\rho}(S_*, \Theta, p), \quad (7)$$

722 both of which are very good fits to the *in situ* density (hence the equals signs); the  
723 increased accuracy of the TEOS-10 equation for density was mostly due to the  
724 refinement of the salinity variable, and the increase in the accuracy of TEOS-10 versus  
725 EOS-80 for Standard Seawater (Millero et al., 2008) was minor by comparison.

726 We need to ask what error will arise from calculating *in situ* density in the model  
727 as  $\tilde{\rho}(S_*/u_{\text{PS}}, \Theta, p)$  instead of as the correct TEOS-10 version of *in situ* density,  $\hat{\rho}(S_*, \Theta, p)$ ?  
728 The effect of this difference on calculations of the buoyancy frequency and even the  
729 neutral tangent plane is likely small, so we concentrate on the effect of this difference on  
730 the isobaric gradient of *in situ* density (the thermal wind).

731 Given that under this Option 2 the model's temperature variable is being  
732 interpreted as Conservative Temperature,  $\Theta$ , the model-calculated isobaric gradient of  
733 *in situ* density is

$$734 \quad \tilde{\rho}_{S_*} \nabla_p S_* + \tilde{\rho}_\theta \nabla_p \Theta, \quad (8)$$

735 whereas the correct isobaric gradient of *in situ* density is actually

$$736 \quad \hat{\rho}_{S_*} \nabla_p S_* + \hat{\rho}_\theta \nabla_p \Theta. \quad (9)$$

737 Notice that here and henceforth we drop the scaling factor  $u_{\text{PS}}$  from the gradient  
738 expressions such as Eqn. (8). In any case, this scaling factor cancels from the expression,  
739 but we simply drop it for ease of looking at the equations; we can imagine that the EOS-  
740 80 equation of state is written in terms of  $S_*$  (which would simply require that a first  
741 line is added to the computer code which divides the salinity variable by  $u_{\text{PS}}$ ).

742 The model's error in evaluating the isobaric gradient of *in situ* density is then the  
743 difference between the two equations above, namely

$$744 \quad \text{error in } \nabla_p \rho = (\tilde{\rho}_{S_*} - \hat{\rho}_{S_*}) \nabla_p S_* + (\tilde{\rho}_\theta - \hat{\rho}_\theta) \nabla_p \Theta. \quad (10)$$

745 The relative error here in the temperature derivative of the equations of state can be  
746 written approximately as

$$747 \quad (\tilde{\rho}_\theta - \hat{\rho}_\theta) / \hat{\rho}_\theta = \tilde{\alpha}^\theta / \hat{\alpha}^\theta - 1, \quad (11)$$

748 which is the difference from unity of the ratio of the thermal expansion coefficient with  
 749 respect to potential temperature to that with respect to Conservative Temperature. This  
 750 ratio,  $\tilde{\alpha}^\theta/\hat{\alpha}^\theta$ , can be shown to be equal to  $c_p(S_*,\theta,0)/c_p^0$  and we know (from Figure 1)  
 751 that this varies by 6% in the ocean. This ratio is plotted in Figure 7(a). In regions of the  
 752 ocean that are very fresh, a relative error in the contribution of the isobaric temperature  
 753 gradient to the thermal wind will be as large as 6% while in most of the ocean this  
 754 relative error will be less than 0.5%.

755 Now we turn our attention to the relative error in the salinity derivative of the  
 756 equation of state, which, from Eqn. (10) can be written approximately as

$$757 \quad \left(\tilde{\rho}_{S_*} - \hat{\rho}_{S_*}\right)/\hat{\rho}_{S_*} = \tilde{\beta}^\theta/\hat{\beta}^\theta - 1, \quad (12)$$

758 and the ratio,  $\tilde{\beta}^\theta/\hat{\beta}^\theta$ , has been plotted (at  $p = 0$  dbar) in Figure 7(b). This figure shows  
 759 that the relative error in the salinity derivative,  $\left(\tilde{\rho}_{S_*} - \hat{\rho}_{S_*}\right)/\hat{\rho}_{S_*}$ , is an increasing  
 760 (approximately quadratic) function of temperature, being approximately zero at 0°C, 1%  
 761 error at 20°C and 2% error at 30°C. An alternative derivation of these implications of  
 762 Eqn. (10) is given in Appendix B.

763 We conclude that under Option 2, where the temperature variable of an EOS-80  
 764 based model (whose polynomial equation of state expects to have potential temperature  
 765 as its input temperature) is interpreted as being Conservative Temperature, there are  
 766 persistent errors in the contribution of the isobaric salinity gradient to the isobaric  
 767 density gradient that are approximately proportional to temperature squared, with the  
 768 error being approximately 1% at a temperature of 20°C (mostly due to the salinity  
 769 derivative of *in situ* density at constant potential temperature being 1% different to the  
 770 corresponding salinity derivative at constant Conservative Temperature). Larger  
 771 fractional errors in the contribution of the isobaric temperature gradient to the thermal  
 772 wind equation do occur (of up to 6%) but these are restricted to the rather small volume  
 773 of the ocean that is quite fresh.

774 In Figure 8 we have evaluated how much the meridional isobaric density  
 775 gradient changes in the upper 1000 dbar of the World Ocean when the temperature  
 776 argument in the expression for density is switched from  $\theta$  to  $\Theta$ . As explained above,  
 777 this switch is almost equivalent to the density difference between calling the EOS-80 and

778 the TEOS-10 equations of state, using the same numeric inputs for each. We find that  
 779 19% of this data has the isobaric density gradient changed by more than 1% when  
 780 switching from  $\theta$  to  $\Theta$ . The median value of the percentage error is 0.22%; that is, 50%  
 781 of the data shallower than 1000 dbar has the isobaric density gradient changed by more  
 782 than 0.22% when switching from using EOS-80 to TEOS-10, with the same numerical  
 783 temperature input, which we are interpreting as being  $\Theta$ .

784 Figure 8 should not be interpreted as being the extra error involved with taking  
 785  $T_{\text{model}}$  to be Conservative Temperature in EOS-80 ocean models, because, due to the lack  
 786 of interior non-conservative source terms, the interpretation of  $T_{\text{model}}$  as being potential  
 787 temperature is already incorrect by an amount that scales as  $\Theta$  minus  $\theta$ . Rather, Figure  
 788 8 illustrates the error in an EOS-80 model due to the use of an equation of state that is  
 789 not appropriate to the way that its temperature variable is treated in the model.

790

### 791 4.3 Evaluating the options for EOS-80 models

792 Under option 1 where  $T_{\text{model}}$  is interpreted as potential temperature, there is a  
 793 non-conservation of heat at the sea surface, with the ocean seeing one heat flux, and the  
 794 atmosphere immediately above it seeing another, with 5% of the differences being larger  
 795 than approximately  $\pm 100 \text{ mW m}^{-2}$ , with a net imbalance of  $16 \text{ mW m}^{-2}$ .

796 Under option 2 where  $T_{\text{model}}$  is interpreted as Conservative Temperature, the air-  
 797 sea flux imbalance does not arise, but two other inaccuracies arise. First, under option 2  
 798 the bulk formulae that determine part of the air-sea flux is based on the surface values of  
 799  $\Theta$  rather than of  $\theta$  (for which the bulk formulae are designed). Second, the isobaric  
 800 density gradient in the upper ocean is typically different by  $\sim 1\%$  to the isobaric density  
 801 gradient that would be found if the TEOS-10 equation of state had been adopted in these  
 802 models. These two aspects of option 2 are considered less serious than not conserving  
 803 heat at the sea surface by up to  $\pm 100 \text{ mW m}^{-2}$ . Neither of the two inaccuracies that arise  
 804 under option 2 are fundamental thermodynamic errors. Rather they are equivalent to  
 805 the ocean modeler choosing (i) a slightly different bulk formulae, and (ii) a slightly  
 806 different equation of state. The constants in the bulk formulae are very poorly known so  
 807 that the switching from  $\theta$  to  $\Theta$  in their use will be well within their uncertainty (Cronin

808 et al., 2019) while the ~1% change to the isobaric density gradient due to using the  
 809 different equations of state is at the level of our knowledge of the equation of state of sea  
 810 water (see the discussion section below).

811 We conclude that option 2 where the  $T_{\text{model}}$  in EOS-80 models is interpreted as  
 812 Conservative Temperature is much preferred as it treats the air-sea heat flux in a manner  
 813 consistent with the First Law of Thermodynamics, and the treatment of  $T_{\text{model}}$  as being a  
 814 conservative variable in the ocean interior is more consistent with it being Conservative  
 815 Temperature than being potential temperature. These same two features of ocean  
 816 models mean that  $T_{\text{model}}$  cannot be accurately interpreted as potential temperature, since  
 817 both the surface flux boundary condition and the lack of the non-conservative source  
 818 terms in the ocean interior mean that these ocean models continually force  $T_{\text{model}}$  away  
 819 from being potential temperature, even if they were initialized as such.

820

## 821 5. Comparison with ocean observations

822 Now that we have argued that  $T_{\text{model}}$  of EOS-80 based models should be  
 823 interpreted as being Conservative Temperature, how then should the model-based  
 824 estimates of ocean heat content and ocean heat flux be compared with ocean  
 825 observations and ocean atlas data? The answer is by evaluating the ocean heat content  
 826 correctly in the observed data sets using TEOS-10, whereby the observed data is used to  
 827 calculate Conservative Temperature, and this is used together with  $c_p^0$  to evaluate ocean  
 828 heat content and meridional heat fluxes.

829 We have made the case that the salinity variable in CMIP ocean models that have  
 830 been spun up for several centuries is Preformed Salinity  $S_*$  for the TEOS-10 compliant  
 831 models, and is  $S_*/u_{\text{ps}}$  for the EOS-80 compliant models. Hence it is the value of either  
 832  $S_*$  or  $S_*/u_{\text{ps}}$  calculated from ocean observations to which the model salinities should be  
 833 compared. Preformed Salinity  $S_*$  is different to Reference Salinity  $S_{\text{R}}$  by only the ratio  
 834  $0.26 = 0.35/1.35$  compared with the difference between Absolute Salinity and Preformed  
 835 Salinity (see Figure 4), and these differences are generally only significantly different to  
 836 zero at depths exceeding 500 m. Note that Preformed Salinity can be evaluated from

837 observations of Practical Salinity using the Gibbs SeaWater (GSW) software  
838 gsw\_Sstar\_from\_SP.

839

## 840 6. Discussion and Recommendations

841 We have made the case that it is advisable to avoid non-conservative sources of  
842 heat at the sea surface. It is the prior interpretation of the temperature variable in EOS-  
843 80 based models as being potential temperature that implies that the ocean receives a  
844 heat flux that is larger by  $\Delta Q$  than the heat that is lost from the atmosphere. Since there  
845 are some areas of the ocean surface where  $\Delta Q$  is as large as the mean rate of global  
846 warming, the issue is important in practice. This realization has motivated the new  
847 interpretation of the prognostic temperature of EOS-80 ocean models as being  
848 Conservative Temperature (our option 2, section 4.2).

849 A consequence of this new interpretation of the prognostic temperature variable  
850 of all CMIP ocean models as being Conservative Temperature means that the EOS-80  
851 based models suffer a relative error of  $\sim 1\%$  in their isobaric gradient of *in situ* density in  
852 the warm upper ocean. How worried should we be about this error? One perspective  
853 on this question is to simply note (from above) that there are larger relative errors  
854 ( $\sim 2.7\%$ ) in the thermal wind equation in the deep ocean due to the neglect of variations  
855 in the relative composition of sea salt. Another perspective is to ask how well science  
856 even knows the thermal expansion coefficient, for example. From appendices K and O  
857 of IOC et al. (2010) (and section 7 of McDougall and Barker (2011)) we see that the RMS  
858 value of the differences between the individual laboratory-based data points of the  
859 thermal expansion coefficient and the thermal expansion coefficient obtained from the  
860 fitted TEOS-10 Gibbs function is  $0.73 \times 10^{-6} \text{ K}^{-1}$  which is approximately 0.5% of a typical  
861 value of the thermal expansion coefficient in the ocean. Without a proper estimation of  
862 the number of degrees of freedom represented by the fitted data points, we might  
863 estimate the relative error of the thermal expansion coefficient obtained from the fitted  
864 TEOS-10 Gibbs function as being half of this, namely 0.25%. So a typical relative error in  
865 the isobaric density gradient of  $\sim 1\%$  in the upper ocean due to using  $\Theta$  rather than  $\theta$  as  
866 the temperature input seems undesirable but not serious.

867           We must also acknowledge that all models have ignored the difference between  
868 Preformed Salinity, Reference Salinity and Absolute Salinity (which is the salinity  
869 variable from which density is accurately calculated). As discussed in IOC et al. (2010),  
870 Wright et al. (2011) and McDougall and Barker (2011), glossing over these issues of the  
871 spatially variable composition of sea salt, which is the same as glossing over the effects  
872 of biogeochemistry on salinity and density, means that all our ocean and climate models  
873 have errors in their thermal wind (vertical shear of horizontal velocity) that globally  
874 exceed 2.7% for half the ocean volume deeper than 1000 m. In the deep North Pacific  
875 Ocean, the misestimation of thermal wind is many times this 2.7% value. The  
876 recommended way of incorporating the spatially varying composition of seawater into  
877 ocean models appears as section A.20 in the TEOS-10 Manual (IOC et al. (2010), and as  
878 section 9 in the McDougall and Barker (2012), with ocean models needing to carry a  
879 second salinity type variable. While it is true that this procedure has the effect of  
880 relaxing the model towards the non-standard seawater composition of today's ocean, it  
881 is clearly advantageous to make a start with this issue by incorporating the non-  
882 conservative source terms that apply to the present ocean rather than to continue to  
883 ignore the issue altogether. As explained in these references, once the modelling of  
884 ocean biogeochemistry matures, the difference between the various types of salinity can  
885 be calculated in real time in an ocean model without the need of referring to historical  
886 data.

887           Nevertheless, we acknowledge that no ocean model to date has attempted to  
888 include the influence of biogeochemistry on salinity and density, and therefore we  
889 recommend that the salinity from both observations and model output be treated as  
890 Preformed Salinity  $S_*$ .

891

### 892 *6.1 Contrasts to the recommendations of Griffies et al. (2016)*

893           How does this paper differ from the recommendations in Griffies et al. (2016)?  
894 That paper recommended that the ocean heat content and meridional transport of heat  
895 should be calculated using the model's temperature variable and the model's value of  
896  $c_p^0$ , and we strenuously agree. However, in the present paper we argue that the

897 temperature variable carried by an EOS-80 based ocean model should be interpreted as  
898 being Conservative Temperature, and not be interpreted as being potential temperature.  
899 This idea was raised as a possibility in Griffies et al. (2016), but the issue was left unclear  
900 in that paper. For example, section D2 of Griffies et al. (2016) recommends that TEOS-10  
901 based models archive potential temperature (as well as their model variable,  
902 Conservative Temperature) “in order to allow meaningful comparisons” with the output  
903 of the EOS-80 based models. We now disagree with this suggestion. The thesis of the  
904 present paper is that the temperature variables of both EOS-80 and TEOS-10 based  
905 models are already directly comparable, and they should both be interpreted as being  
906 Conservative Temperature, and they should both be compared with Conservative  
907 Temperature from observations. The fact that the model's temperature variable is  
908 labelled "thetao" in EOS-80 models and "bigthetao" in TEOS-10 based models we now  
909 see as very likely to cause confusion, since we are recommending that the temperature  
910 outputs of both types of ocean models should be interpreted as Conservative  
911 Temperature.

912 The present paper also diverges from Griffies et al. (2016) in the way that the  
913 salinity variables in CMIP ocean models should be interpreted and thus compared to  
914 observations. Griffies et al. (2016) interpret the salinity variable in TEOS-10 based ocean  
915 models as being Reference Salinity  $S_R$  whereas we show that these models actually  
916 carry Preformed Salinity  $S_*$  but have errors in their calculation of densities. Similarly,  
917 Griffies et al. (2016) interpret the salinity variable in EOS-80 based ocean models as being  
918 Practical Salinity  $S_p$  whereas we show that these models actually carry  $S_*/u_{ps}$ , that is,  
919 Preformed Salinity divided by the constant,  $u_{ps}$ . This distinction between the present  
920 paper and Griffies et al. (2016) is negligible in the upper ocean where Preformed Salinity  
921 is almost identical to Reference Salinity (because the composition of seawater in the  
922 upper ocean is close to Reference Composition), but in the deeper parts of the ocean, the  
923 distinction is not negligible; for example, based on the work of McCarthy et al. (2015) we  
924 have shown that the use of Absolute Salinity versus Preformed Salinity leads to ~1 Sv  
925 difference in the meridional overturning streamfunction in the North Atlantic at a depth  
926 of 2700 m. However, in this deeper part of the ocean, even though the difference

927 between Absolute Salinity and Preformed Salinity is not negligible, the difference  
 928 between Preformed Salinity and Reference Salinity (which the TEOS-10 based ocean  
 929 models have to date assumed their salinity variable to be) is smaller in the ratio  $0.35/1.35$   
 930  $= 0.26$  (see Figure 4). That is, if the salinity output of a TEOS-10 based ocean model was  
 931 taken to be Reference Salinity, the error would be only a quarter of the difference  
 932 between Absolute Salinity and Preformed Salinity, a difference which limits the  
 933 accuracy of the isobaric density gradients in the deeper parts of ocean models (see  
 934 Figure 4). A similar remark applies to EOS-80 based ocean models if their salinity  
 935 output is regarded as being Practical Salinity instead of being (as we propose)  $S_*/u_{PS}$ .

936

### 937 *6.2 Summary table of ocean heat content imbalances*

938 In Table 1 we summarize the effects of uncertainties in physical or numerical processes  
 939 in estimating ocean heat content or its changes. The first two rows are the rate of  
 940 warming (expressed in  $\text{mWm}^{-2}$  averaged over the sea surface) due to anthropogenic  
 941 global warming, and due to geothermal heating. The third row is an estimate of the  
 942 surface heat flux equivalent of the depth-integrated rate of dissipation of turbulent  
 943 kinetic energy, and the fourth is an estimate of the neglected net flux of potential  
 944 enthalpy at the sea surface due to the evaporation and precipitation of water occurring  
 945 at different temperatures.

946 The next (fifth) row is the consequence of considering the scenario where all the  
 947 radiant heat is absorbed into the ocean at a pressure of 25 dbar rather than at the sea  
 948 surface. The derivative of specific enthalpy with respect to Conservative Temperature at  
 949 25 dbar,  $\hat{h}_\theta$ , is  $c_p^0$  times the ratio of the absolute in situ temperature at 25 dbar,  $(T_0 + t)$ ,  
 950 to the absolute potential temperature,  $(T_0 + \theta)$  at this pressure (see Eqn. (A.11.15) of IOC  
 951 et al. (2010)). The ratio of  $\hat{h}_\theta$  to  $c_p^0$  at 25 dbar is typically different to unity by  $6 \times 10^{-6}$ ,  
 952 and taking a typical rate of radiative heating of  $100 \text{ Wm}^{-2}$  over the ocean's surface leads  
 953 to  $0.6 \text{ mWm}^{-2}$  as the area-averaged rate of mis-estimation of the surface flux of  
 954 Conservative Temperature for this assumed pressure of penetrative radiation. Since this  
 955 is so small, the use of  $c_p^0$  (rather than  $\hat{h}_\theta$ ) to convert the divergence of the radiative heat  
 956 flux into a flux of Conservative Temperature is well supported, providing the correct



957 diagnostics are used for the calculation (such diagnostic issues may be responsible for  
 958 the heat budget closure issues identified by Irving et al. 2020).

959 The next six rows of Table 1 list the mean and twice the standard deviation of the  
 960 volume integrated non-conservation production of Conservative Temperature, potential  
 961 temperature, and specific entropy, all expressed in  $\text{mWm}^{-2}$  at the sea surface. The  
 962 following two rows are the results we have found in this paper for the air-sea heat flux  
 963 error that is made if the EOS-80's temperature is taken to be potential temperature.

964 The final three rows show that ocean models, being cast in flux divergence form  
 965 with heat fluxes being passed between one grid box and the next, do not have  
 966 appreciable numerical errors in deducing air-sea fluxes from changes in the volume  
 967 integrated heat content.

968 The estimate from Graham and McDougall (2013) of  $-10 \text{ mWm}^{-2}$  is for the net  
 969 interior production of  $\theta$ , so this is a net destruction. A steady state requires this amount  
 970 of extra flux of  $\theta$  at the sea surface (so it can be consumed in the interior). Our estimate  
 971 of this extra flux of  $\theta$  at the sea surface is  $16 \text{ mWm}^{-2}$ , which is only a little larger than the  
 972 estimate of Graham and McDougall (2013).

973

### 974 *6.3 Summary of recommendations*

975 In summary, this paper has argued for the following guidelines for analyzing the  
 976 CMIP model runs. We should

- 977 1. interpret the prognostic temperature variable of all CMIP models (whether they  
 978 are based on the EOS-80 or the TEOS-10 equation of state) as being Conservative  
 979 Temperature,
- 980 2. compare the model's prognostic temperature with the Conservative  
 981 Temperature,  $\Theta$ , of observational data,
- 982 3. calculate the ocean heat content as the volume integral of the product of  
 983 (i) in situ density (for non-Boussinesq models or reference density for  
 984 Boussinesq) (ii) the model's prognostic temperature,  $\Theta$ , and (iii) the model's  
 985 value of  $c_p^0$ ,

- 986 4. interpret the salinity variable of the model output as being Preformed Salinity  $S_*$   
 987 for TEOS-10 based ocean models, and  $S_*/u_{ps}$  for EOS-80 based ocean models (so  
 988 it is advisable to post-multiply the salinity output of EOS-80 models by  $u_{ps}$  in  
 989 order to have the salinity outputs of all types of CMIP models as Preformed  
 990 Salinity  $S_*$ ) and,  
 991 5. compare the model's salinity variable with Preformed Salinity,  $S_*$ , calculated  
 992 from ocean observations.  
 993 6. Sea surface temperature should be taken as the model's prognostic temperature  
 994 in the case of EOS-80 models (since this is the temperature that was used in the  
 995 bulk formulae), and as the calculated and stored values of potential temperature  
 996 in the case of TEOS-10 models.  
 997 7. Ensure that all required fixed variables, such as  $c_p^0$ , (boussinesq) reference  
 998 density, seawater volume, and freezing equation are saved to the CMIP archives  
 999 alongside the prognostic temperature and salinity variables, so that analysts have  
 1000 all components required to accurately interpret the model fields. In addition,  
 1001 providing the full-depth OHC timeseries for each simulation would provide a  
 1002 quantified target for analysts to compare and contrast changes across models and  
 1003 simulations.

1004 Note that this sixth recommendation for EOS-80 based models exposes an unavoidable  
 1005 inconsistency in that the surface values of the model's prognostic temperature is best  
 1006 regarded internally in the ocean model as being Conservative Temperature, but we  
 1007 cannot avoid the fact that this same temperature was used as the sea surface (*in situ*)  
 1008 temperature in the bulk formulae during the running of such ocean models. Issues such  
 1009 as these will not arise when all ocean models have been converted to the TEOS-10  
 1010 equation of state.

1011 How then should the model's salinity and temperature outputs,  $S_*$  and  $\Theta$ , be used to  
 1012 evaluate dynamical concepts such as streamfunctions, dynamic height, etc? The answer  
 1013 most consistent with the running of a numerical model is to use the equation of state  
 1014 that the model used, together with the model's temperature and salinity outputs on the  
 1015 native grid of the model. This method is important when studying detailed dynamical

1016 balances in ocean model output. But since we now have the output salinity and  
1017 temperature of both EOS-80 and TEOS-10 models being the same (namely  $S_*$  and  $\Theta$ ),  
1018 there is an efficiency and simplicity argument to analyze the output of all these models  
1019 in the same manner, using algorithms from the Gibbs SeaWater (GSW) Oceanographic  
1020 Toolbox of TEOS-10 (McDougall and Barker, 2011). Doing these model inter-  
1021 comparisons often involves interpolating the model outputs to different depths (or  
1022 pressures) than those used in the original ocean model, so incurring some interpolation  
1023 errors. While the use of the GSW software means that the *in situ* density will be  
1024 calculated slightly differently than in some of the forward models, thus affecting the  
1025 thermal wind and sea-level rise, these differences are small, as can be seen by comparing  
1026 Figures A.5.1 and A.5.2 of the TEOS-10 Manual, IOC et al. (2010). Hence it is viable for  
1027 most purposes to evaluate density and dynamic height using the GSW Oceanographic  
1028 Toolbox, with the input salinity to this GSW code being the model's Preformed Salinity,  
1029 and the temperature input being the Conservative Temperature, which as we have  
1030 argued, are the model's prognostic variables.

1031 Another issue that may arise is where a TEOS-10 based model has been run with  
1032 Conservative Temperature, but the monthly-mean Conservative Temperature output  
1033 has been converted into potential temperature before sending the model output to the  
1034 CMIP archive. What is the damage done if this inaccurately averaged value of potential  
1035 temperature is converted back to Conservative Temperature using only the monthly-  
1036 mean potential temperature and salinity? While such an issue is perhaps an operational  
1037 detail that takes us some distance from our intention of writing an academic paper about  
1038 these issues, nevertheless we show Figure 9 which indicates that transforming between  
1039 these monthly-averaged values is not a serious issue.

1040

#### 1041 **Author Contribution**

1042 T J McD. devised this new way of interpreting CMIP ocean model variables, P. M. B and  
1043 R. M. H. provided figures for the paper, and all authors contributed to the concepts and  
1044 the writing of the manuscript.

1045

1046 **Acknowledgements.** We have benefitted from helpful comments and suggestions from  
1047 Drs. Baylor Fox-Kemper, Sjoerd Groeskamp, Casimir de Lavergne, John Krasting, Fabien  
1048 Roquet, Geoff Stanley, and Jan-Erik Tesdal. This paper contributes to the tasks of the  
1049 Joint SCOR/IAPSO/IAPWS Committee on the Thermophysical Properties of Seawater.  
1050 T. J. McD, P. M. B and R. M. H. gratefully acknowledge Australian Research Council  
1051 support through grant FL150100090. The work of P.J.D. was prepared by Lawrence  
1052 Livermore National Laboratory (LLNL) under contract no. DE-AC52-07NA27344.  
1053

1054 **Appendix A: A non-seawater thermodynamic interpretation of Option 1**

1055 Ocean models have always assumed a constant isobaric heat capacity, and have  
 1056 traditionally assumed that the model's temperature variable is whatever temperature  
 1057 the equation of state was designed to accept. Here we enquire whether there is a way of  
 1058 justifying Option 1 thermodynamically in the sense that Option 1 would be totally  
 1059 consistent with thermodynamic principles for a fluid that is different to real seawater.

1060 That is, we pursue the idea that these EOS-80 based ocean models are not  
 1061 actually models of seawater, but are models of a slightly different fluid. We require a  
 1062 fluid that is identical to seawater in some respects, such as that it has the same dissolved  
 1063 material (Millero et al., 2008) and the same issues around Absolute Salinity, Preformed  
 1064 Salinity and Practical Salinity, and the same in situ density as real seawater (at given  
 1065 values of Absolute Salinity, potential temperature and pressure). But we require that the  
 1066 expression for the enthalpy of this new fluid is different to that of real seawater.

1067 The difference that we envisage between real seawater and this new fluid is that,  
 1068 at zero pressure, the enthalpy of the new fluid is given exactly by the constant value  $c_p^0$   
 1069 times potential temperature  $\theta$ . That is, for the new fluid, potential enthalpy  $h^0$  is  
 1070 simply  $c_p^0\theta$  (as it would be for an ideal gas), and the air-sea interaction for this new fluid  
 1071 would be exactly as it occurs in the EOS-80 based models. Moreover, conservation of  
 1072 potential temperature is justified for this new fluid, and the density and thermal wind  
 1073 would also be correctly evaluated in these EOS-80 based models.

1074 The enthalpy of this new fluid is then given by (since  $h_p = v$ )

$$1075 \quad \tilde{h}(S_A, \theta, p) = c_p^0 \theta + \int_{P_0}^P \tilde{v}(S_A, \theta, p') dp', \quad (\text{A1})$$

1076 while the entropy of this new fluid needs to obey the consistency relationship,  
 1077  $\tilde{\eta}_\theta = \tilde{h}_\theta(p=0)/(T_0 + \theta)$ , which reduces to

$$1078 \quad \tilde{\eta}_\theta = \frac{c_p^0}{(T_0 + \theta)}, \quad (\text{A2})$$

1079 where  $T_0 = 273.15$  K is the Celsius zero point. This consistency relationship is derived  
 1080 directly from the Fundamental Thermodynamic Relationship (see Table P.1 of IOC et al.,

1081 2010). Integrating Eqn. (A2) with respect to potential temperature at constant salinity  
 1082 leads to the following expression for entropy that our new fluid must obey,

$$1083 \quad \tilde{\eta}(S_A, \theta) = c_p^0 \ln\left(1 + \frac{\theta}{T_0}\right) + a \left(\frac{S_A}{S_{SO}}\right) \ln\left(\frac{S_A}{S_{SO}}\right). \quad (A3)$$

1084 The variation here with salinity is taken from the TEOS-10 Gibbs-function-derived  
 1085 expression for specific entropy which contains the last term in Eqn. (A3) with the  
 1086 coefficient  $a$  being  $a = -9.310292413479596 \text{ J kg}^{-1} \text{ K}^{-1}$  (this is the value of the coefficient  
 1087 derived from the  $g_{110}$  coefficient of the Gibbs function (appendix H of IOC *et al.* (2010)),  
 1088 allowing for our version of the normalization of salinity,  $(S_A/S_{SO})$ ). This term was  
 1089 derived by Feistel (2008) to be theoretically correct at vanishingly small Absolute  
 1090 Salinities.

1091 With these definitions, Eqns. (A1) and (A3), of enthalpy and entropy of our new  
 1092 fluid, we have completely defined all the thermophysical properties of the fluid (see  
 1093 Appendix P of IOC *et al.*, 2010 for a discussion). Many aspects of the fluid are different  
 1094 to seawater, including the adiabatic lapse rate (and hence the relationship between in  
 1095 situ and potential temperatures), since the adiabatic lapse rate is given by  $\Gamma = \tilde{h}_{\theta P} / \tilde{\eta}_{\theta}$   
 1096 and while the numerator is the same as for seawater (since  $\tilde{h}_{\theta P} = \tilde{h}_{\theta P} = \tilde{v}_{\theta}$ ), the  
 1097 denominator,  $\tilde{\eta}_{\theta}$ , which is now given by Eqn. (A2), can be up to 6% different to the  
 1098 corresponding function,  $\tilde{\eta}_{\theta}$ , appropriate to real seawater.

1099 We conclude that this is indeed a conceptual way of forcing the EOS-80 based  
 1100 models to be consistent with thermodynamic principles. That is, we have shown that  
 1101 these EOS-80 models are not models of seawater, but they do accurately model a  
 1102 different fluid whose thermodynamic definition we have given in Eqns. (A1) and (A3).  
 1103 This new fluid interacts with the atmosphere in the way that EOS-80 models have  
 1104 assumed to date, the potential temperature of this new fluid is correctly mixed in the  
 1105 ocean in a conservative fashion, and the equation of state is written in terms of the  
 1106 model's temperature variable, namely potential temperature.

1107 Hence we have constructed a fluid which is different thermodynamically to  
 1108 seawater, but it does behave exactly as these EOS-80 models treat their model seawater.  
 1109 That is, we have constructed a new fluid which, if seawater had these thermodynamic

1110 characteristics, then the EOS-80 ocean models would have correct thermodynamics,  
1111 while being able to interpret the model's temperature variable as being potential  
1112 temperature.

1113         But this does not change the fact that in order to make these EOS-80 models  
1114 thermodynamically consistent in this way we have ignored the real variation at the sea  
1115 surface of the isobaric specific heat capacity; a variation that we know can be as large as  
1116 6%.

1117         Hence we do not propose this non-seawater explanation as a useful  
1118 rationalization of the behaviour of EOS-80 based ocean models. Rather, it seems less  
1119 dramatic and more climatically relevant to adopt the simpler interpretation of Option 2.  
1120 Under this option we accept that the model is modelling actual seawater, that the  
1121 model's temperature variable is in fact Conservative Temperature, and that there are  
1122 some errors in the equation of state of these EOS-80 models that amount to errors of the  
1123 order of 1% in the thermal wind relation throughout much of the upper (warm) ocean.  
1124 That is, so long as we interpret the temperature variable of these EOS-80 based models  
1125 as Conservative Temperature, they are fine except that they have used an incorrect  
1126 equation of state; they have used  $\tilde{\rho}$  rather than  $\hat{\rho}$ . Apart from this "error" in the ocean  
1127 code, Option 2 is a consistent interpretation of the ocean model thermodynamics and  
1128 dynamics. In ocean models there are always questions of how to parameterize ocean  
1129 mixing. To this uncertain aspect of ocean physics, under Option 2 we add the less than  
1130 desirable expression that is used to evaluate density in EOS-80 based ocean models in  
1131 CMIP

1132

1133

1134 **Appendix B: An alternative derivation of Eqn. (10)**

1135 Eqn. (10) is an expression for the error in the isobaric density gradient when  
 1136 Conservative Temperature is used as the input temperature variable to the EOS-80  
 1137 equation of state (which expects its input temperature to be potential temperature). An  
 1138 alternative accurate expression to Eqn. (9) for the isobaric density gradient is

$$1139 \quad \tilde{\rho}_{S_*} \nabla_p S_* + \tilde{\rho}_\theta \nabla_p \theta, \quad (\text{B1})$$

1140 and subtracting this from the incorrect expression, Eqn. (8), gives the following  
 1141 expression for the model's error in evaluating the isobaric gradient of in situ density,

$$1142 \quad \text{error in } \nabla_p \rho = \tilde{\rho}_\theta \nabla_p (\Theta - \theta). \quad (\text{B2})$$

1143 An approximate fit to the temperature difference,  $\Theta - \theta$ , as displayed in Figure 2 is

$$1144 \quad (\Theta - \theta) \approx 0.05 \Theta \left( 1 - \frac{S_A}{S_{SO}} \right) - 1.75 \times 10^{-3} \Theta \left( 1 - \frac{\Theta}{25^\circ\text{C}} \right), \quad (\text{B3})$$

1145 and using this approximate expression in the right-hand side of Eqn. (B2) gives

$$1146 \quad \frac{\text{error in } \nabla_p \rho}{\tilde{\rho}_\theta} \approx \left[ 0.05 \left( 1 - \frac{S_*}{S_{SO}} \right) - 1.75 \times 10^{-3} \left( 1 - \frac{\Theta}{12.5^\circ\text{C}} \right) \right] \nabla_p \Theta - \frac{0.05}{S_{SO}} \Theta \nabla_p S_* . \quad (\text{B4})$$

1147 The first part of this expression that multiplies  $\nabla_p \Theta$  corresponds to the proportional  
 1148 error in the thermal expansion coefficient displayed in Figure 7(a). The second part of  
 1149 Eqn. (B4) amounts to an error in the saline derivative of the equation of state, with the  
 1150 proportional error (corresponding to Eqn. (12)), being  $-0.05 \tilde{\rho}_\theta \Theta / (\hat{\rho}_{S_A} S_{SO})$ , and this is  
 1151 close to the error that can be seen in Figure 7(b). This error is approximately a quadratic  
 1152 function of temperature since the thermal expansion coefficient  $\tilde{\rho}_\theta$  is approximately a  
 1153 linear function of temperature.

1154

1155

1156



1157  
1158

	Heat flux contributions of different processes	$\text{mWm}^{-2}$
Physical processes	Global warming imbalance (Zanna et al., 2019), mean	<b>+300</b>
	Geothermal heating (Emile-Geay and Madec, 2009), mean	<b>+86</b>
	Viscous dissipation (Graham and McDougall, 2013), mean	<b>+3</b>
	Atmospheric water fluxes of enthalpy (Griffies et al. 2016), mean	<b>-(150-300)</b>
Non-conservation errors	Extra flux of $\theta$ if the air-sea radiative heat flux is taken to occur at a pressure of 25dbar	<b>-0.6</b>
	non-conservation of $\theta$ (Graham & McDougall 2013), mean	<b>+0.3</b>
	non-conservation of $\theta$ (Graham & McDougall 2013), $2^*\text{rms}$	<b>+1</b>
	non-conservation of $\theta$ (Graham & McDougall 2013), mean	<b>-10</b>
	non-conservation of $\theta$ (Graham & McDougall 2013), $2^*\text{rms}$	$\pm$ <b>120</b>
	non-conservation of $\eta$ (Graham & McDougall 2013), mean	<b>+380</b>
	non-conservation of $\eta$ (Graham & McDougall 2013), $2^*\text{rms}$	<b>+1200</b>
	Interpreting EOS-80 T as $\theta$ (ACCESS-CM2 estimate), mean	<b>+16</b>
	Interpreting EOS-80 T as $\theta$ (ACCESS-CM2 estimate), $2^*\text{rms}$	$\pm$ <b>135</b>
Numerical errors	ACCESS-OM2 single time-step	$\pm$ <b><math>10^{-7}</math></b>
	ACCESS-OM2 diagnosed from OHC snapshots	$\pm$ <b>0.001</b>
	ACCESS-CM2 diagnosed from OHC monthly-averages	$\pm$ <b>0.03</b>

1159  
1160

1161 **Table 1:** Summary of the impact of various processes and modelling errors on the global  
1162 ocean heat budget and its imbalance. All numbers are in units of  $\text{mWm}^{-2}$ . Numerical errors  
1163 are diagnosed from either ACCESS-OM2 (machine precision errors) or ACCESS-CM2  
1164 (associated with not having access to OHC snapshots). Numbers from interior processes are  
1165 converted to equivalent surface fluxes by depth integration. The sign convention here is that a  
1166 positive heat flux is heat entering the ocean, or warming the ocean by internal dissipation. The  
1167 symbol  $\eta$  in this table stands for entropy.

1168

1169 **Code Availability**

1170 This paper has not run any ocean or climate models, and so has not produced any  
1171 such computer code. Processed data and code to produce the ACCESS-CM2 figures 5,  
1172 6 and 9 is located at the github repository

1173 [https://github.com/rmholmes/ACCESS\\_CM2\\_SpecificHeat](https://github.com/rmholmes/ACCESS_CM2_SpecificHeat).

1174

1175

1176 **Data Availability**

1177 This paper has not produced any model data. Processed data and code to produce the  
1178 ACCESS-CM2 figures 5, 6 and 9 is located at the github repository

1179 [https://github.com/rmholmes/ACCESS\\_CM2\\_SpecificHeat](https://github.com/rmholmes/ACCESS_CM2_SpecificHeat).

1180

1181

1182

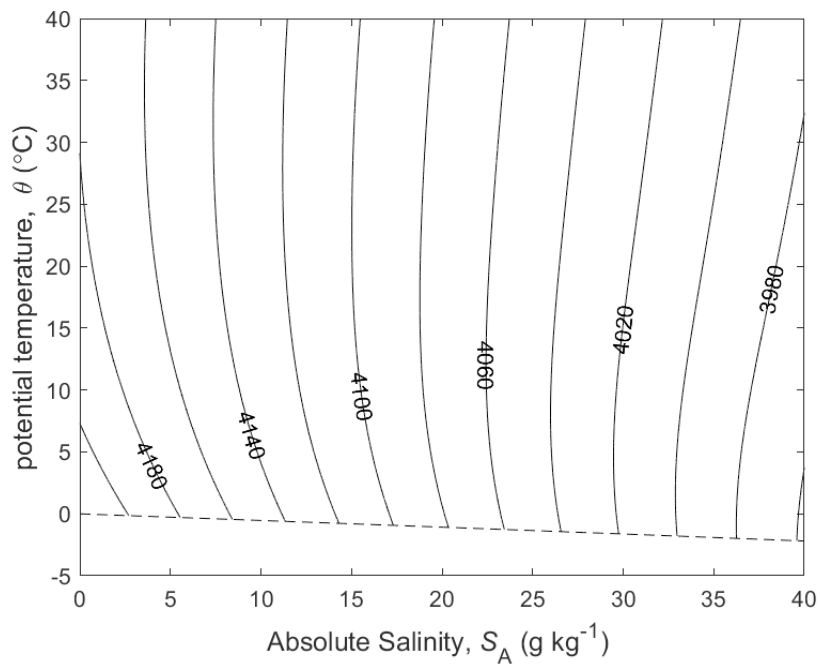
1183 **References**

- 1184 Bi, D., Dix, M., Marsland, S., O'Farrell, S., Rashid, H., Uotila, P., Hirst, A., Kowalczyk, E.,  
 1185 Golebiewski, M., Sullivan, A., Yan, H., Hannah, N., Franklin, C., Sun, Z., Vohralik, P.,  
 1186 Watterson, I., Zhou, X., Fiedler, R., Collier, M., Ma, Y., Noonan, J., Stevens, L., Uhe, P.,  
 1187 Zhu, H., Griffies, S., Hill, R., Harris, C. and Puri, K.: The ACCESS coupled model:  
 1188 description, control climate and evaluation, *Aust. Met. Oceanogr. J.*, **63**, 41-64, 2013.
- 1189 Cronin M. F., Gentemann C. L., Edson J., Ueki I., Bourassa M., Brown S., Clayson C. A.,  
 1190 Fairall C. W., Farrar J. T., Gille S. T., Gulev S., Josey S. A., Kato S., Katsumata M., Kent  
 1191 E., Krug M., Minnett P. J., Parfitt R., Pinker R. T., Stackhouse P. W., Swart S., Tomita H.,  
 1192 Vandemark D., Weller A. R., Yoneyama K., Yu L., Zhang D.: Air-Sea Fluxes With a  
 1193 Focus on Heat and Momentum. *Frontiers in Marine Science*, **6**, 430.  
 1194 <https://www.frontiersin.org/article/10.3389/fmars.2019.00430> , 2019.
- 1195 Emile-Geay J. and Madec G.: Geothermal heating, diapycnal mixing and abyssal circulation.  
 1196 *Ocean Science*, **5**, 203-217, 2019.
- 1197 Feistel, R.: A Gibbs function for seawater thermodynamics for  $-6$  to  $80$  °C and salinity up to  
 1198  $120 \text{ g kg}^{-1}$ , *Deep-Sea Res. I*, **55**, 1639-1671, 2008.
- 1199 Feistel, R., Wright D. G., Kretzschmar H.-J., Hagen E., Herrmann S. and Span R.:  
 1200 Thermodynamic properties of sea air. *Ocean Science*, **6**, 91–141. [http://www.ocean-](http://www.ocean-sci.net/6/91/2010/os-6-91-2010.pdf)  
 1201 [sci.net/6/91/2010/os-6-91-2010.pdf](http://www.ocean-sci.net/6/91/2010/os-6-91-2010.pdf) , 2010.
- 1202 Graham, F. S. and McDougall T. J.: Quantifying the non-conservative production of  
 1203 Conservative Temperature, potential temperature and entropy. *Journal of Physical*  
 1204 *Oceanography*, **43**, 838-862. <http://dx.doi.org/10.1175/JPO-D-11-0188.1> , 2013.
- 1205 Griffies, S. M., Danabasoglu, G., Durack, P. J., Adcroft, A. J., Balaji, V., Böning, C. W.,  
 1206 Chassignet, E. P., Curchitser, E., Deshayes, J., Drange, H., Fox-Kemper, B., Gleckler, P.  
 1207 J., Gregory, J. M., Haak, H., Hallberg, R. W., Heimbach, P., Hewitt, H. T., Holland, D.  
 1208 M., Ilyina, T., Jungclaus, J. H., Komuro, Y., Krasting, J. P., Large, W. G., Marsland, S. J.,  
 1209 Masina, S., McDougall, T. J., Nurser, A. J. G., Orr, J. C., Pirani, A., Qiao, F., Stouffer, R.  
 1210 J., Taylor, K. E., Treguier, A. M., Tsujino, H., Uotila, P., Valdivieso, M., Wang, Q.,  
 1211 Winton, M., and Yeager, S. G.: OMIP contribution to CMIP6: experimental and  
 1212 diagnostic protocol for the physical component of the Ocean Model Intercomparison

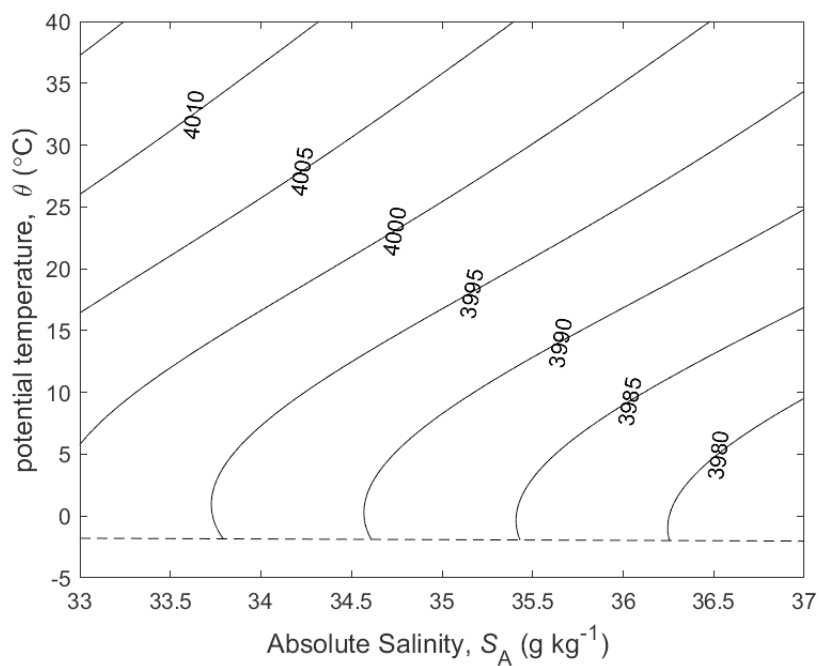
- 1213 Project: *Geosci. Model Dev.*, **9**, 3231-3296, doi:10.5194/gmd-9-3231-2016.
- 1214 <http://dx.doi.org/10.5194/gmd-9-3231-2016> , 2016.
- 1215 IOC, SCOR and IAPSO: *The international thermodynamic equation of seawater – 2010:*
- 1216 *Calculation and use of thermodynamic properties*. Intergovernmental Oceanographic
- 1217 Commission, Manuals and Guides No. 56, UNESCO (English), 196 pp. available at
- 1218 [http://www.TEOS-10.org/pubs/TEOS-10\\_Manual.pdf](http://www.TEOS-10.org/pubs/TEOS-10_Manual.pdf) Many of the original papers on
- 1219 which TEOS-10 is based were published in the following Special Issue of *Ocean Science*,
- 1220 [https://os.copernicus.org/articles/special\\_issue14.html](https://os.copernicus.org/articles/special_issue14.html) 2010.
- 1221 Irving, D., Hobbs W., Church J. and Zika J.: A Mass and Energy Conservation Analysis of
- 1222 Drift in the CMIP6 Ensemble. *Journal of Climate*, **34**, 3157-3170,
- 1223 <https://doi.org/10.1175/JCLI-D-20-0281.1>, 2021.
- 1224 Jackett, D. R. and McDougall T. J.: Minimal adjustment of hydrographic profiles to achieve
- 1225 static stability. *Journal of Atmospheric and Oceanic Technology*, **12**, 381-389.
- 1226 [https://journals.ametsoc.org/doi/abs/10.1175/1520-](https://journals.ametsoc.org/doi/abs/10.1175/1520-0426%281995%29012%3C0381%3AMA0HPT%3E2.0.CO%3B2)
- 1227 [0426%281995%29012%3C0381%3AMA0HPT%3E2.0.CO%3B2](https://journals.ametsoc.org/doi/abs/10.1175/1520-0426%281995%29012%3C0381%3AMA0HPT%3E2.0.CO%3B2) , 1995.
- 1228 McCarthy, G.D., Smeed, D.A., Johns, W.E., Frajka-Williams, E., Moat, B.I., Rayner, D.,
- 1229 Baringer, M.O., Meinen, C.S., Collins, J. and Bryden, H.L.: Measuring the Atlantic
- 1230 Meridional Overturning Circulation at 26°N. *Progress in Oceanography*, **130**, 91-111.
- 1231 [doi:10.1016/j.pocean.2014.10.006](https://doi.org/10.1016/j.pocean.2014.10.006) , 2015.
- 1232 McDougall, T. J.: Potential enthalpy: A conservative oceanic variable for evaluating heat
- 1233 content and heat fluxes. *Journal of Physical Oceanography*, **33**, 945-963.
- 1234 <https://journals.ametsoc.org/jpo/article/33/5/945/10023/> , 2003.
- 1235 McDougall T. J. and Barker P. M.: *Getting started with TEOS-10 and the Gibbs Seawater*
- 1236 *(GSW) Oceanographic Toolbox*, 28pp, SCOR/IAPSO WG127, ISBN 978-0-646-55621-5.
- 1237 available at [http://www.TEOS-10.org/pubs/Getting\\_Started.pdf](http://www.TEOS-10.org/pubs/Getting_Started.pdf) , 2011.
- 1238 McDougall, T. J., Church J. A. and Jackett, D. R.: Does the nonlinearity of the equation
- 1239 of state impose an upper bound on the buoyancy frequency? *Journal of Marine*
- 1240 *Research*, **61**, 745-764, <http://dx.doi.org/10.1357/002224003322981138> , 2003.
- 1241 McDougall, T. J. and Feistel R.: What causes the adiabatic lapse rate? *Deep-Sea Research I*,
- 1242 **50**, 1523-1535. <http://dx.doi.org/10.1016/j.dsr.2003.09.007> , 2003.

- 1243 McDougall, T. J., Jackett D. R., Millero F. J., Pawlowicz R. and Barker P. M.: A global  
1244 algorithm for estimating Absolute Salinity. *Ocean Science*, **8**, 1123-1134.  
1245 <http://www.ocean-sci.net/8/1123/2012/os-8-1123-2012.pdf> , 2012.
- 1246 Millero, F. J., Feistel R., Wright D. G. and McDougall T. J.: The composition of Standard  
1247 Seawater and the definition of the Reference-Composition Salinity Scale. *Deep-Sea*  
1248 *Research-I*, **55**, 50-72. <http://dx.doi.org/10.1016/j.dsr.2007.10.001> , 2008.
- 1249 Pawlowicz, R.: A model for predicting changes in the electrical conductivity, Practical Salinity,  
1250 and Absolute Salinity of seawater due to variations in relative chemical composition. *Ocean*  
1251 *Science*, **6**, 361–378. <http://www.ocean-sci.net/6/361/2010/os-6-361-2010.pdf> , 2010.
- 1252 Pawlowicz, R.: The Absolute Salinity of seawater diluted by riverwater. *Deep-Sea Research I*,  
1253 **101**, 71-79, 2015.
- 1254 Pawlowicz, R., Wright D. G. and Millero F. J.: The effects of biogeochemical processes on  
1255 oceanic conductivity/salinity/density relationships and the characterization of real seawater.  
1256 *Ocean Science*, **7**, 363–387. <http://www.ocean-sci.net/7/363/2011/os-7-363-2011.pdf>, 2011.
- 1257 Pawlowicz, R., McDougall T., Feistel R. and Tailleux R.: An historical perspective on the  
1258 development of the Thermodynamic Equation of Seawater – 2010: *Ocean Sci.*, **8**, 161-  
1259 174. <http://www.ocean-sci.net/8/161/2012/os-8-161-2012.pdf> , 2012.
- 1260 Roquet, F., Madec G., McDougall T. J. and Barker P. M.: Accurate polynomial expressions for  
1261 the density and specific volume of seawater using the TEOS-10 standard. *Ocean*  
1262 *Modelling*, **90**, 29-43. <http://dx.doi.org/10.1016/j.ocemod.2015.04.002> , 2015.
- 1263 Tailleux, R.: Identifying and quantifying nonconservative energy production/destruction terms  
1264 in hydrostatic Boussinesq primitive equation models. *Ocean Modelling*, **34**, 125-136,  
1265 <https://doi.org/10.1016/j.ocemod.2010.05.003> , 2010.
- 1266 Tailleux, R.: Observational and energetics constraints on the non-conservation of  
1267 potential/Conservative Temperature and implications for ocean modelling. *Ocean*  
1268 *Modelling*, **88**, 26-37. <https://doi.org/10.1016/j.ocemod.2015.02.001> , 2015.
- 1269 von Schuckmann, K. et al. Heat stored in the Earth system: where does the energy go? *Earth*  
1270 *Syst. Sci. Data*, **12**, 2013-2041, 2020.
- 1271 Wright, D. G., Pawlowicz R., McDougall T. J., Feistel R. and Marion G. M.: Absolute Salinity,  
1272 “Density Salinity” and the Reference-Composition Salinity Scale: present and future use

- 1273 in the seawater standard TEOS-10. *Ocean Sci.*, **7**, 1-26. <http://www.ocean->  
1274 [sci.net/7/1/2011/os-7-1-2011.pdf](http://www.ocean-sci.net/7/1/2011/os-7-1-2011.pdf), 2011.
- 1275 Young, W.R., Dynamic Enthalpy, Conservative Temperature, and the Seawater Boussinesq  
1276 Approximation, *Journal of Physical Oceanography*, **40**, 394-400,  
1277 doi: 10.1175/2009JPO4294.1 , 2010.
- 1278 Zanna L., Khatiwala S., Gregory J. M., Ison, J. and Heimbach P.: Global reconstruction of  
1279 historical ocean heat storage and transport, *Proceedings of the National Academy of*  
1280 *Sciences*, **116**, 1126-1131, 2019.
- 1281  
1282

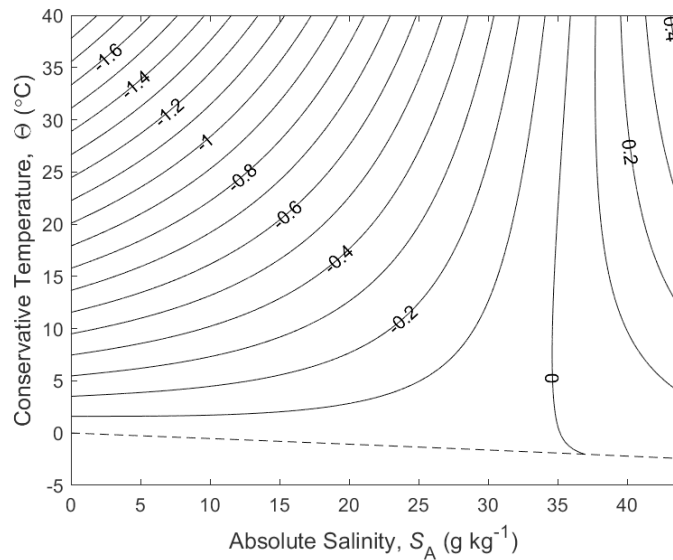


1283



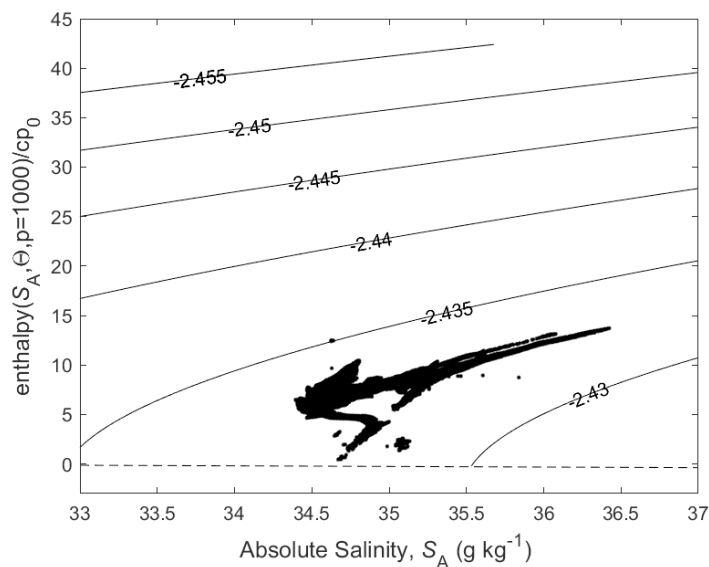
1284  
 1285  
 1286  
 1287  
 1288

**Figure 1.** (a) Contours of isobaric specific heat capacity  $c_p$  of seawater (in  $\text{J kg}^{-1} \text{K}^{-1}$ ), at  $p = 0$  dbar. (b) a zoomed-in version for a smaller range of Absolute Salinity. The dashed line is the freezing line at  $p = 0$  dbar.



1289  
1290  
1291  
1292  
1293

**Figure 2.** Contours (in  $^{\circ}\text{C}$ ) of the difference between potential temperature and Conservative Temperature,  $\theta - \Theta$ .



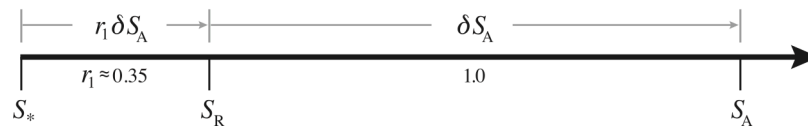
1294  
1295

**Figure 3.** Contours of  $\Theta - \hat{h}(S_A, \Theta, 1000\text{dbar}) / c_p^0$  on the Absolute Salinity –  $\hat{h}(S_A, \Theta, 1000\text{dbar}) / c_p^0$  diagram. Enthalpy,  $\hat{h}(S_A, \Theta, 1000\text{dbar})$ , is a conservative quantity for turbulent mixing processes that occur at a pressure of 1000dbar. The mean value of the contoured quantity is approximately  $-2.44^{\circ}\text{C}$  illustrating that enthalpy does not possess the “potential” property; that is, enthalpy increases during adiabatic and isohaline increases in pressure. The fact that the contoured quantity on this figure is not a linear function of  $S_A$  and  $\hat{h}(S_A, \Theta, 1000\text{dbar})$  illustrates the (small) non-conservative nature of Conservative Temperature. The dots are data from the world ocean at 1000dbar.

1296  
1297  
1298  
1299  
1300  
1301  
1302  
1303  
1304  
1305



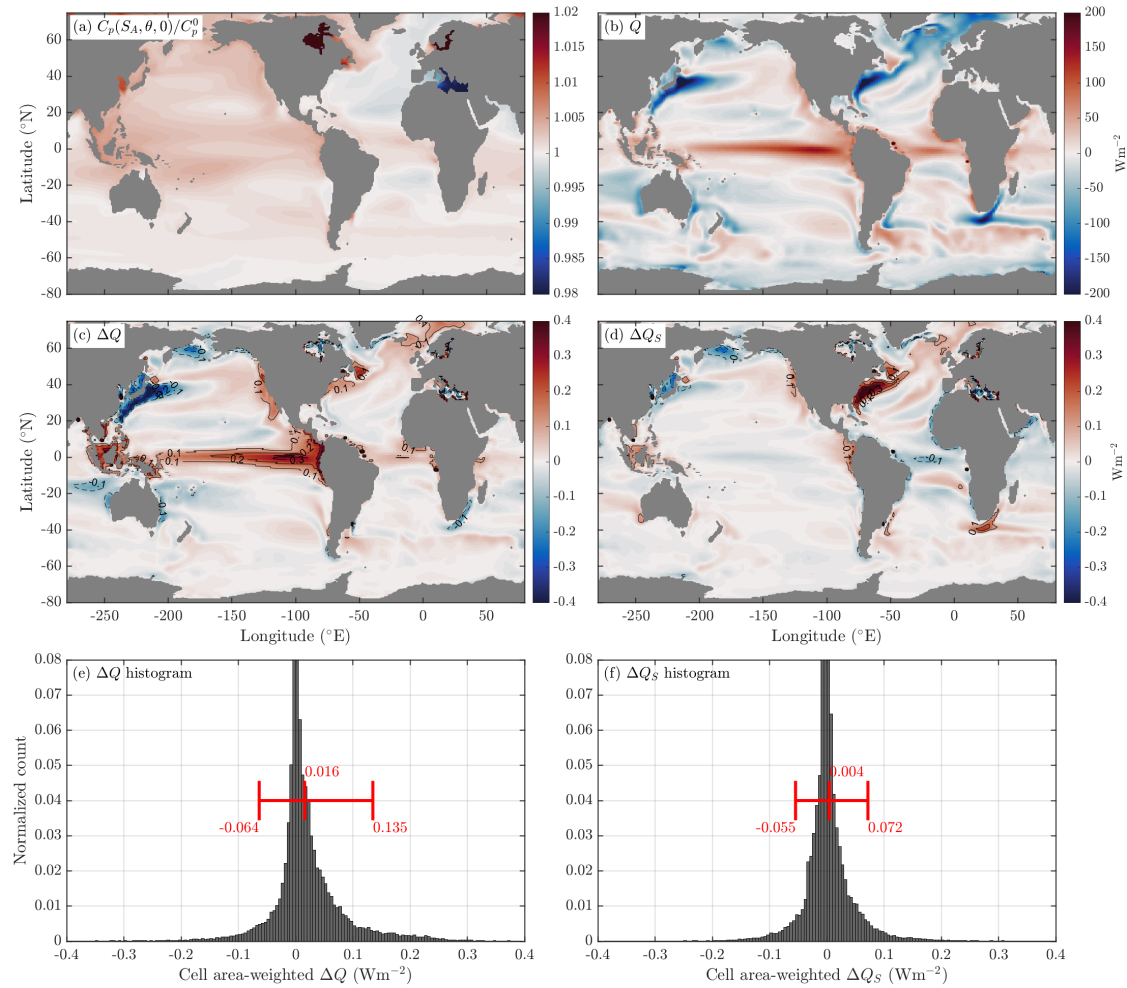
1306  
1307  
1308  
1309



1310  
1311  
1312  
1313  
1314  
1315  
1316  
1317  
1318  
1319

**Figure 4.** Number line of salinity, illustrating the differences between Preformed Salinity  $S_*$ , Reference Salinity  $S_R$ , and Absolute Salinity  $S_A$  for seawater whose composition differs from that of Standard Seawater which has Reference Composition. If a seawater sample has Reference Composition, then  $\delta S_A = 0$  and  $S_*$ ,  $S_R$  and  $S_A$  are all equal.

1320

1321  
1322

1323

1324

1325

1326

1327

1328

1329

1330

1331

1332

1333

1334

1335

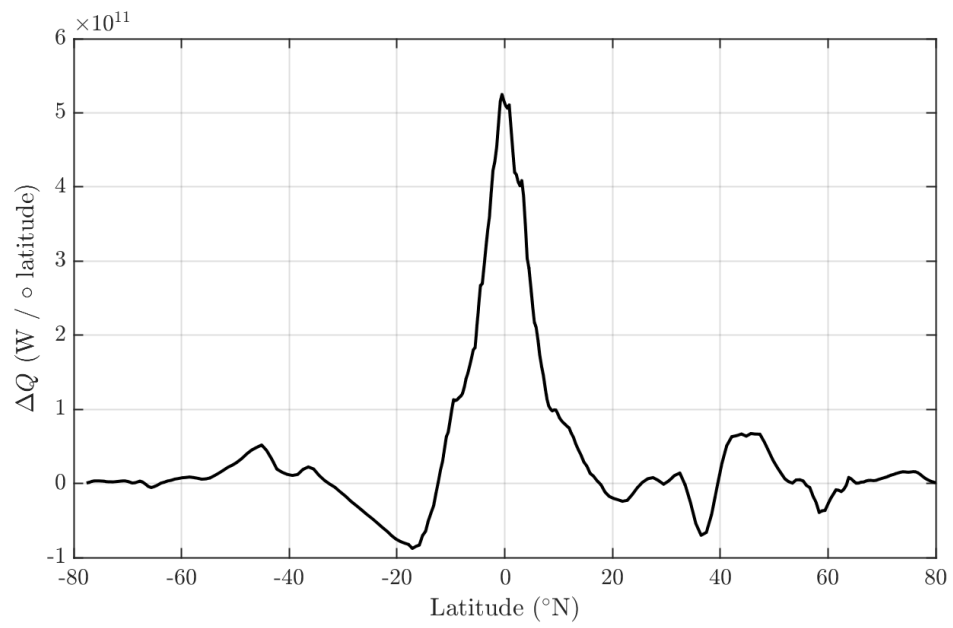
1336

1337

1338

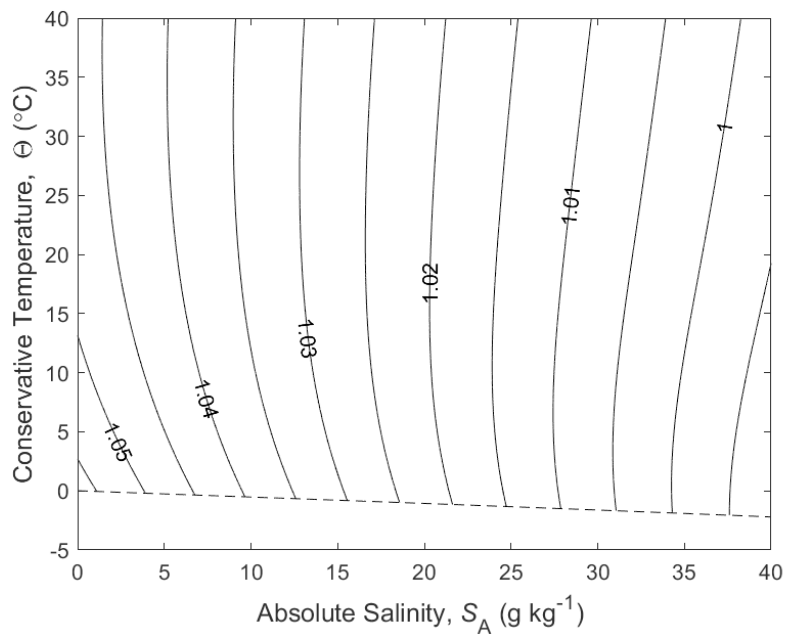
1339

**Figure 5.** (a) The average value of the ratio of the isobaric specific heat of seawater and  $c_p^0$  for data from the ACCESS-CM2 model's pre-industrial control simulation (600 years long). (b) The average surface heat flux  $Q$  ( $\text{Wm}^{-2}$ ) in this same ocean model. (c) The additional heat that the ocean receives/loses compared to the heat that the atmosphere loses/receives (assuming that an EOS-80 model's temperature variable is potential temperature),  $\Delta Q$  ( $\text{Wm}^{-2}$ , Eqn. 6). (e) a histogram of  $\Delta Q$  weighted by the area of each grid cell. (d) The contribution of salinity variations to the air-sea heat flux discrepancy, given by  $\Delta Q_S = Q(S - \bar{S})(1/c_p^0)\partial c_p/\partial S$ , where  $\bar{S}$  is the surface mean salinity and  $\partial c_p/\partial S$  is the variation in the specific heat with salinity at the surface mean salinity and potential temperature. (f) a histogram of  $\Delta Q_S$  weighted by the area of each grid cell. Shown in red in panels e and f are the mean, 5<sup>th</sup> and 95<sup>th</sup> percentiles of the histogram ( $\text{Wm}^{-2}$ ). Note that these calculations neglect correlations between surface properties and the surface heat flux at sub-monthly time scales.

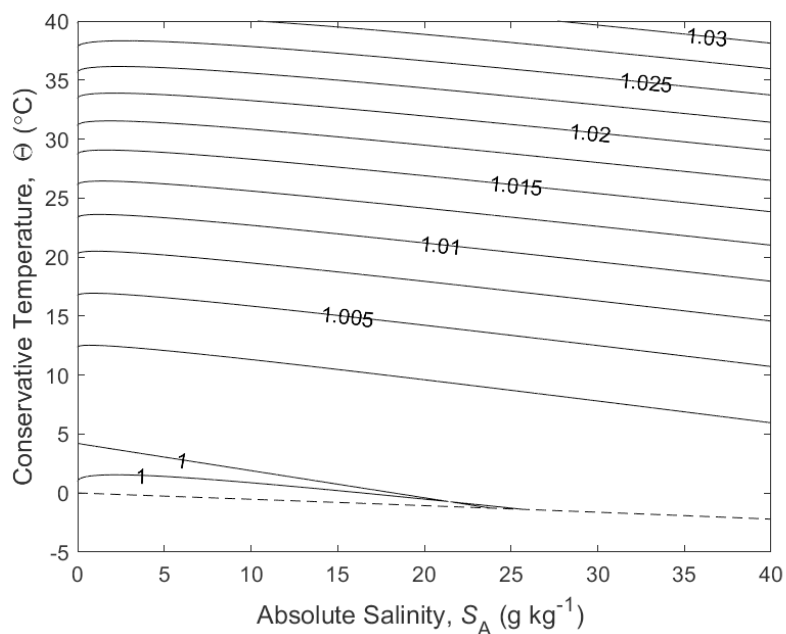


1340  
1341  
1342  
1343  
1344  
1345

**Figure 6.** The ACCESS-CM2 zonally integrated  $\Delta Q$  From Fig.5c, showing the imbalance in the air-sea heat flux in Watts per degree of latitude.



1346



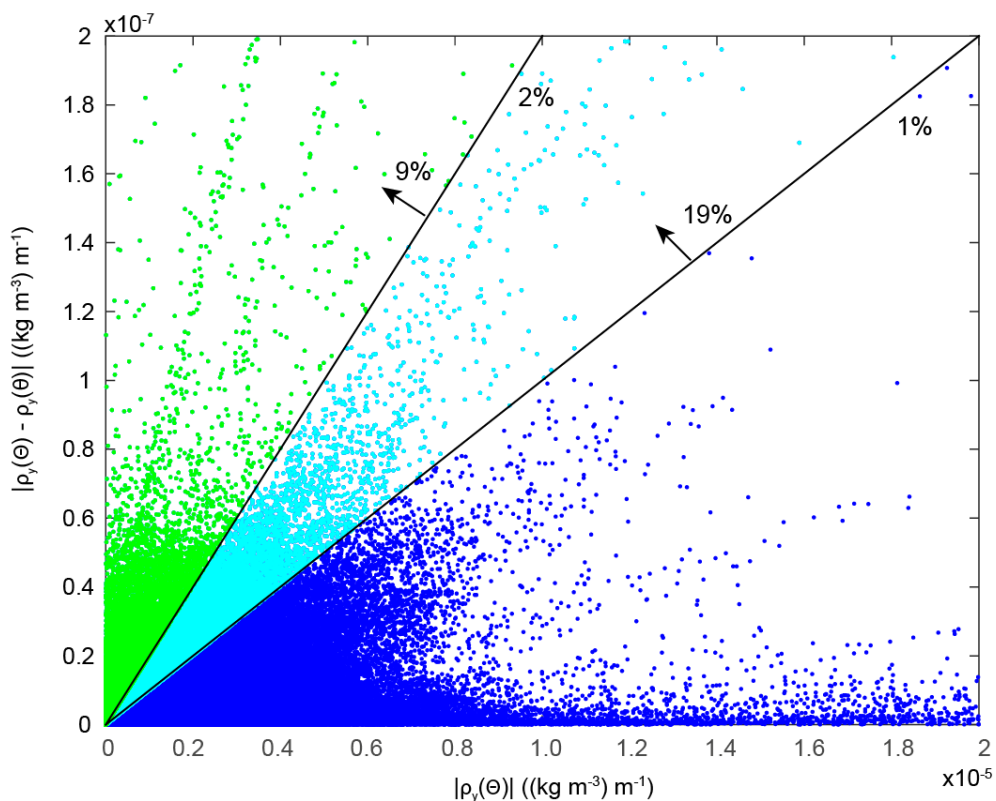
1347

1348

1349 **Figure 7.** (a) The ratio of the thermal expansion coefficients with respect to Conservative  
 1350 Temperature and potential temperature,  $\tilde{\alpha}^\theta / \hat{\alpha}^\Theta = \tilde{\Theta}_\theta$ . (b) The ratio of the saline  
 1351 contraction coefficients at constant potential temperature to that at constant Conservative  
 1352 Temperature,  $\tilde{\beta}^\theta / \hat{\beta}^\Theta = 1 + (\hat{\alpha}^\Theta / \hat{\beta}^\Theta) \hat{\theta}_{S,} / \hat{\theta}_\Theta$  at  $p = 0$  dbar.

1353

1354



1355

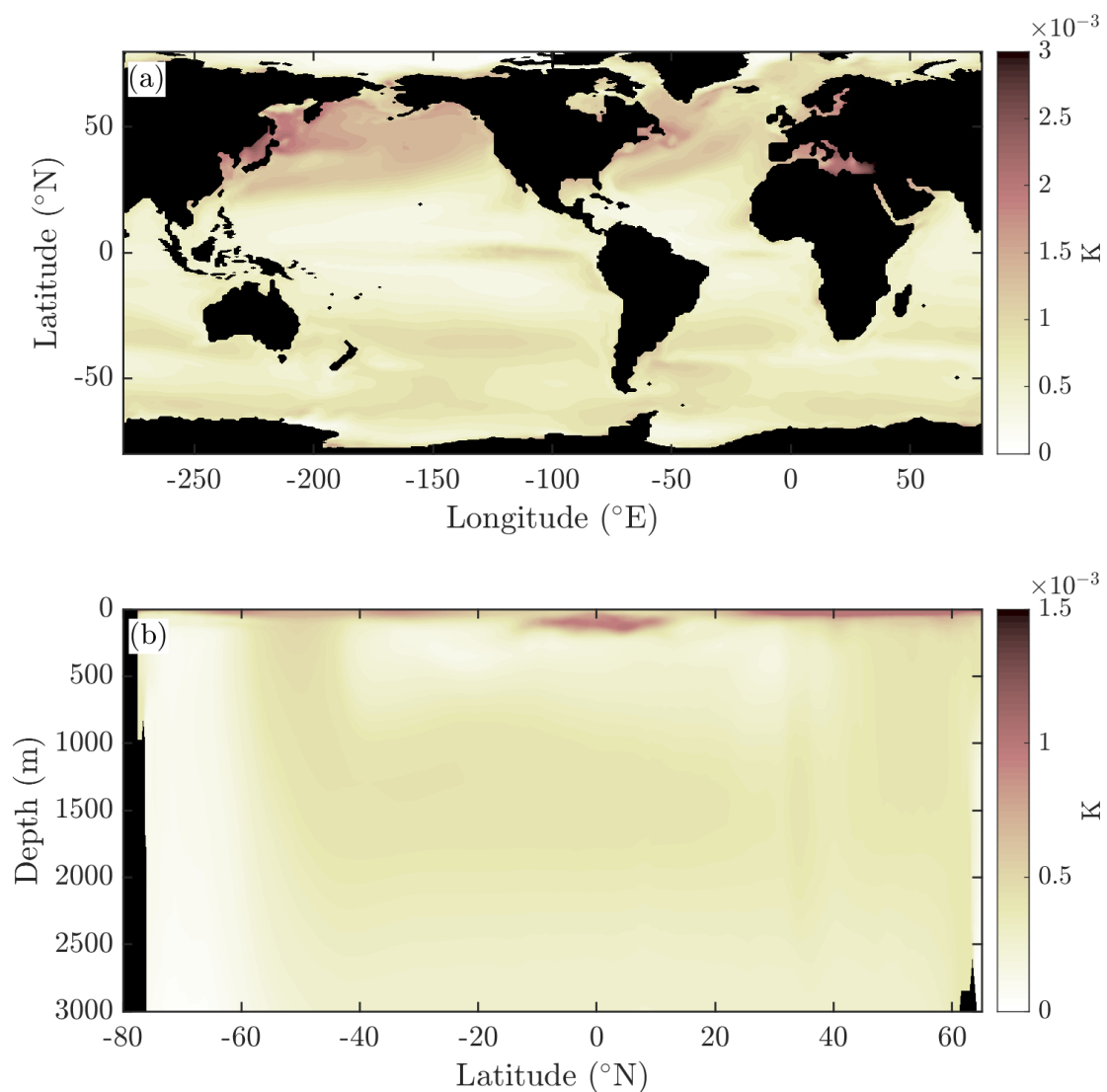
1356

**Figure 8.** The northward density gradient at constant pressure (the horizontal axis) for data in the global ocean atlas of Gouretski and Koltermann (2004) for  $p < 1000$  dbar. The vertical axis is the magnitude of the difference between evaluating the density gradient using  $\Theta$  versus  $\theta$  as the temperature argument in the expression for density. This is virtually equivalent to the density difference between calling the EOS-80 and the TEOS-10 equations of state, using the same numeric inputs for each. The 1% and 2% lines indicate where the isobaric density gradient is in error by 1% and 2%. 19% of the data shallower than 1000 dbar has the isobaric density gradient changed by more than 1% when switching between the equations of state. The median value of the percentage error in the isobaric density gradient is 0.22%.

1366

1367

1368



1369  
 1370  
 1371  
 1372  
 1373  
 1374  
 1375  
 1376  
 1377  
 1378

**Figure 9.** The RMS error (K) in evaluating Conservative Temperature from the CMIP6 archived monthly-averaged values of potential temperature and salinity, compared with averaging the instantaneous values of Conservative Temperature for a month at the (a) surface and (b) the zonal mean. These quantities are calculated from 50 years of temporally averaged output from the ACCESS-CM2 model's pre-industrial control simulation. The errors are seen to be no larger than a few mK.